



1 **From substrate to soil in a pristine environment –**  
2 **pedochemical, micromorphological and microbiological**  
3 **properties from soils on James Ross Island, Antarctica**

4  
5 Lars A. Meier<sup>1\*</sup>, Patryk Krauze<sup>2\*</sup>, Isabel Prater<sup>3</sup>, Fabian Horn<sup>2</sup>, Carlos E.G.R. Schaefer<sup>4</sup>,  
6 Thomas Scholten<sup>1</sup>, Dirk Wagner<sup>2, 5</sup>, Carsten W. Mueller<sup>3</sup>, and Peter Kühn<sup>1</sup>

7 <sup>1</sup>Department of Geosciences, University of Tuebingen, Tuebingen, D-72070, Germany

8 <sup>2</sup>GFZ German Research Centre for Geosciences, Section Geomicrobiology, Potsdam, D-14473, Germany

9 <sup>3</sup>Lehrstuhl für Bodenkunde, TU München, Freising, D-85354, Germany

10 <sup>4</sup>Departamento de Solos, Universidade Federal de Viçosa, Viçosa, BR-36571-000, Brazil

11 <sup>5</sup>Institute for Earth and Environmental Sciences, University of Potsdam, Potsdam, D-14476, Germany

12 *Correspondence to:* Lars A. Meier ([lars-arne.meier@uni-tuebingen.de](mailto:lars-arne.meier@uni-tuebingen.de))

13 \*shared first authorship

14

15

16

17

18

19

20

21

22

23

24

25

26

27

28

29

30

31

32

33

34

35

36

37

38

39



40 **Abstract.** James Ross Island (JRI) offers the exceptional opportunity to study pedogenesis  
41 without the influence of vascular plants or faunal activities (e.g. penguin rookeries) in a  
42 landscape marking the transition from maritime to continental Antarctica. Here, primarily  
43 microbial communities control soil biological processes and affect soil chemical and physical  
44 properties in a semiarid region with mean annual precipitation from 200 to 500mm and mean  
45 air temperature below 0°C. The impact of climate change on soil forming processes in this part  
46 of Antarctica and its related microbial processes is unknown. In this study, two soil profiles  
47 from JRI (one at St. Martha Cove - SMC, and another at Brandy Bay - BB) were investigated  
48 by combining pedological, geochemical and microbiological methods. The soil profiles are  
49 similar in respect to topographic position and parent material but are spatially separated by an  
50 orographic barrier and therefore represent lee- and windward locations towards the mainly  
51 south-westerly winds. Opposing trends in the depth functions of pH and differences in EC-  
52 values are caused by additional input of bases by sea spray at BB, the site close to the Prince  
53 Gustav Channel. Both soils are classified as Cryosols, dominated by bacterial taxa such as  
54 Actinobacteria, Proteobacteria, Acidobacteria, Gemmatimonadates and Chloroflexi. A shift in  
55 the dominant taxa in both soils and an increased abundance of multiple operational taxonomic  
56 units (OTUs) related to potential chemolithoautotrophic Acidiferrobacteraceae was observed.  
57 This shift was accompanied by a change in soil microstructure below 20cm depth, with potential  
58 impact on water availability and matter fluxes. Multivariate statistics revealed correlations  
59 between the microbial community structure and soil parameters such as chloride, sulfate,  
60 calcium and organic carbon contents, grain size distribution, as well as the pedogenic oxide  
61 ratio.

62  
63  
64  
65  
66  
67  
68  
69  
70  
71  
72  
73  
74  
75  
76



## 77 1 Introduction

78 In extreme environments, like Antarctica, local climatic conditions such as low temperatures,  
79 precipitation or irradiance are important and often limiting factors for soil formation. Even  
80 though soils in Antarctica are often poorly developed, they can be highly diverse (Michel et al.,  
81 2014; Simas et al., 2008; Bockheim et al., 2015). Therefore, soil scientific investigations  
82 became a relevant topic in Antarctic research, proofing that there are actually soils in Antarctica  
83 (Jensen, 1916) and identifying soil forming processes (Ugolini, 1964). Antarctic soil research  
84 is mostly located in Victoria Land, continental Antarctica, especially in the McMurdo Dry  
85 Valleys (Michel et al., 2014; Ugolini and Bockheim, 2008), in the South Shetlands, maritime  
86 Antarctica (Simas et al., 2015) and the western Antarctic Peninsula Region (APR) (Haus et al.,  
87 2015; Hrbáček et al., 2017b; Schaefer et al., 2017; Souza et al., 2014; Pereira et al., 2017).

88 Soils from continental Antarctica are often saline with thick salt horizons (Souza et al., 2014).  
89 Due to environmental stressors such as very low temperatures, low water availability, frequent  
90 freeze-thaw cycles and limited organic nutrient contents, soils from continental Antarctica show  
91 limiting conditions for life (Cary et al., 2010). Nevertheless, suitable edaphic niches like cryptic  
92 and refuge habitats, microbial mats and permafrost soils exist that harbor microbial  
93 communities (Cowan et al., 2014).

94 Soils in maritime Antarctica and western APR differ from soils in continental Antarctica  
95 according to their stage of development (Balks et al., 2013; Blume et al., 2004; Parnikoza et al.,  
96 2017). They show extensive cryoturbation processes with occasional salt crusts at the soil  
97 surface (Balks et al., 2013; Bockheim, 1997). Local conditions determine nutrient availability  
98 in soils, with Ca, Mg, K and P contents being in general high on igneous, volcanic rocks,  
99 whereas P and N contents are highest in ornithogenic soils.

100 Soils from the eastern part of the APR (also called Weddell Sea sector) are different, since they  
101 are associated with a dry climatic transitional zone between the wet, warmer maritime  
102 Antarctica and colder, arid continental Antarctica. Mean temperatures are below 0°C and liquid  
103 water supply is sufficient to allow soil forming processes (Souza et al., 2014). Souza et al.  
104 (2014) also showed that cryoturbation is less pronounced in the eastern APR than in the South  
105 Shetlands. The base saturation (>50%) and electric conductivity (EC) are generally high  
106 whereas the amount of total organic carbon (TOC) is substantially low. Regarding  
107 cryoturbation, active layer depth, chemical weathering and soil organic C-content, soils from  
108 the eastern APR are comparable to soils from inland areas of the Ross Sea Region (Balks et al.,  
109 2013), though they are formed on different parent material (Daher et al., 2018). In comparison,  
110 the transitional zone of the eastern APR with semiarid soils remains one of the least studied  
111 areas in Antarctica (Souza et al., 2014; Daher et al., 2018).

112 Since Microorganisms in Antarctica show a broad diversity as revealed by recent molecular  
113 phylogenetic and metagenomic methods (Cowan et al., 2014) and contribute to the weathering  
114 of minerals in soils (Uroz et al., 2009), they are pivotal to understand initial soil formation. The  
115 bacterial phyla Proteobacteria, Acidobacteria, Actinobacteria, Bacteroidetes, Firmicutes and  
116 Gemmatimonadates, commonly found in temperate soils, also dominate the microbial



117 communities observed in Antarctic habitats (e.g. Bajerski and Wagner, 2013; Cary et al., 2010;  
118 Pearce et al., 2012; Chong et al., 2012). The microbial community structure is influenced by  
119 local soil chemical parameters, especially pH (e.g. Chong et al., 2010, Siciliano et al., 2014),  
120 but also by soil physical parameters such as grain size distribution and soil moisture (Ganzert  
121 et al., 2011). Chong et al. (2015) proposed, however, that historical contingency and dispersal  
122 limitations could have a stronger influence on differences in community distributions at a  
123 regional scale (>1000km). Ganzert et al. (2011) found that at a small scale, microbial activity  
124 has a distinct influence on soil chemical parameters and, therefore, on its microbial  
125 composition. Conflicting results illustrate the lack in the understanding of drivers of soil  
126 microbial diversity in high latitude soils (Cowan et al., 2014).

127 Micromorphological studies in the maritime Antarctica and the western APR described  
128 sulphurization and phosphatization in ornithogenic soils and mineral transformation on  
129 volcanic rocks (Pereira et al., 2013; Schaefer et al., 2008); and paleosols (Kirshner and  
130 Anderson, 2011; Spinola et al., 2017). Even though micromorphology offers the opportunity to  
131 study constituents of soil and their mutual relations in space and time and to identify soil  
132 forming processes in an undisturbed state (Stoops, 2003), so far no micromorphological study  
133 has been published about soil forming processes in the eastern APR that are influenced neither  
134 by sulfates nor by birds.

135 Our study sites are located on James Ross Island in the eastern APR and therefore offers a  
136 unique setting to study soil formation and microbial communities in a transitional Antarctic  
137 landscape between the wet maritime and dry, colder continental Antarctica. We selected two  
138 different soils, representing coastal soils and inland soils of James Ross Island, developed on  
139 similar substrate and at similar topographic positions. *Our study aims to identify major soil and  
140 microbiological properties, not influenced by vascular plants, sulfides and penguin rookeries,  
141 and their respective depth function and interplays, by combining pedochemical and  
142 micromorphological methods with microbial community studies based on high throughput  
143 sequence analyses.*

## 144 **2. Regional setting of James Ross Island, maritime Antarctica**

145 James Ross Island is situated east of the Antarctic Peninsula and is the largest island in the  
146 western Weddell Sea sector (Hjort et al., 1997). The study area is located on Ulu Peninsula in  
147 the northern part of JRI (Fig. 1). It represents one of the largest ice-free areas of the APR  
148 (Nedbalová et al., 2013; Hrbáček et al., 2017b) with the beginning of its deglaciation  $12.9 \pm 1.2$   
149 ka ago (Nývlt et al., 2014). More than 300 km<sup>2</sup> of the JRI lowlands are currently ice-free, except  
150 for a few glaciers (Engel et al., 2012).

151

152 **[ Figure 1 ]**

153

154 The climate on JRI is semi-arid polar-continental (Martin and Peel, 1978). The precipitation,  
155 mostly snow, ranges between 200 to 500 mm of water equivalent per year with the major share



156 during winter (Davies et al., 2013; Zvěřina et al., 2014). The thickness of the snow cover does  
157 not exceed 30 cm, but varies due to strong winds (Hrbáček et al., 2017b; Hrbáček et al., 2016a).  
158 The annual air temperature ranges between +10 °C and -30 °C on Ulu Peninsula (Hrbáček et  
159 al., 2016a; Láska et al., 2011). The year 2015 marked the warmest summer ever measured on  
160 Ulu Peninsula, having a mean seasonal summer temperature (MSST) of 0.0 °C and a maximum  
161 air temperature of 13.3 °C (Hrbáček et al., 2017a); even though the mean annual air temperature  
162 (MAAT) decreased slightly from -6.8 °C in 2011 to -7°C in 2015 (Hrbáček et al., 2016b; Láska  
163 et al., 2012).

164 The two study sites are located at Brandy Bay (BB) near the western coast and at St. Martha  
165 Cove (SMC) at the eastern coast of Ulu Peninsula. Both sites are located at similar topographic  
166 positions (small plateaus) and elevation (80 m a.s.l.) with no visible vegetation (Fig. 2 and Fig.  
167 3).

168

169 [ **Figure 2** ]

170 [ **Figure 3** ]

171

172 BB is located windward towards the mainly south-westerly winds (Hrbáček et al., 2016c; Nývlt  
173 et al., 2016), whereas SMC is located leeward, shielded by the Lachman Crags from the stronger  
174 winds. This results in less precipitation in the eastern part of JRI (Davies et al., 2013). Therefore,  
175 BB can be considered as a characteristic wind-exposed coastal site with high influence of sea  
176 spray, whereas SMC represents a characteristic soil of an inland site with less influence of sea  
177 spray.

178 The substrate of both study sites is basically composed of coarse-grained cretaceous sandstones  
179 and siltstones of the Alpha Member of the Santa Martha Formation (Hrbáček et al., 2017b).  
180 The land surface is generally covered by a debris layer of gravels and large clasts mixed with  
181 loose sandy regolith, mostly derived from James Ross Volcanic Group basalts, which were  
182 deposited as debris flows containing mainly basalt and hyaloclastite breccia and palagonite  
183 (Davies et al., 2013; Hrbáček et al., 2017b; Salzmänn et al., 2011). No nesting birds are found  
184 on JRI.

185 The continuous permafrost on James Ross Island shows an active layer thickness ranging  
186 between 40 and 107 cm related to the topographic position on Ulu Peninsula (Bockheim et al.,  
187 2013; Borzotta and Trombotto, 2004).

### 188 **3. Material and Methods**

#### 189 **3.1 Soil sampling**

190 During the austral summer period in 2016 soil samples from BB and SMC (Fig. 4 and Fig. 5)  
191 were taken. The amount of coarse material bigger than 2mm was larger at the profile from BB,  
192 due to strong wind ablation. The permafrost table was not reached in both soil profiles, but  
193 ground ice was visible in a depth of 85cm at SMC, whereas no ice was found in BB. Both



194 profiles were dug until a layer of coarse gravel was found. Bulk samples of both profiles were  
195 taken in depth increments (0-5cm, 5-10cm, 10-20cm, 20-50cm, >50cm) and were placed into  
196 sterile plastic bags, which were frozen immediately. Continuous cooling at -20°C was ensured  
197 by a transfer with the research vessels *RV Polarstern* to Germany. For micromorphological  
198 analyses, undisturbed and oriented samples were taken in modified Kubiena boxes (10cm x  
199 6cm x 5cm). Samples for micromorphology were taken at depth of 0-10cm, 10-20cm, 30-40cm,  
200 50-60cm and 80-90cm at SMC. BB samples represent the depth of 10-20cm, 20-30cm und 40-  
201 50cm. Soils were described according to Food and Agriculture Organization of the United  
202 Nations (FAO) (2006) and classified according to the World Reference Base for Soil Resources  
203 (WRB; IUSS Working Group WRB, 2015).

204

205 [ Figure 4 ]

206 [ Figure 5 ]

## 207 3.2 Soil physical and chemical analysis

### 208 3.2.1 Grain size distribution

209 The samples were saturated (100ml of deionized water) and sonicated (800J ml<sup>-1</sup>). Coarse-  
210 medium sand (>200µm), fine sand (63-200µm) and coarse silt (20-63µm) were obtained by wet  
211 sieving. The smaller fractions, including medium silt (6.3-20µm), fine silt (2-6.3µm) and clay  
212 (<2µm), were separated by sedimentation. Fractions >20µm were dried at 45°C and weighed  
213 afterwards. The fractions <20µm were freeze-dried before weighing. The different procedures  
214 were chosen due to practical reasons: freeze-drying allows submitting the finer fractions to  
215 further analyses (particularly carbon and nitrogen content) immediately, while the coarser  
216 fractions need milling anyway.

### 217 3.2.2 pH, EC, C&N contents, major elements and pedogenic oxides

218 The pH value was obtained using a pH meter (ph197i, WTW, Germany). Electrical conductivity  
219 was measured with a conductivity meter (LE703, Mettler-Toledo, USA). Values of pH and  
220 electric conductivity were measured from bulk samples < 2mm in deionized water with a  
221 sample to solution ratio of 1:2.5.

222 Carbon (C) and nitrogen (N) contents of the bulk soils were analyzed by dry combustion  
223 (Elementar CNS Vario Max Cube). 300 to 500mg per sample were analyzed in duplicate. The  
224 inorganic carbon content was determined by acid fumigation after Ramnarine et al. (2011). 100  
225 mg of the milled bulk soil samples were moistened with 20 to 40 µl of deionized water and put  
226 into a desiccator together with 100ml of 37% HCl. Afterwards, the samples were dried at 40°C  
227 and weighed. Finally, C<sub>inorg</sub> content was measured by dry combustion (EuroVector  
228 EuroEA3000 Elemental Analyser).

229 Major elements were analysed with a wavelength dispersive XRF device (AXS S4 Pioneer,  
230 Bruker, USA). Prior to preparation, the samples (ratio Li-metaborate to soil 1:5) were ground



231 with an agate mill for 12 minutes. Major elements were used for the calculation of weathering  
232 indices.

233 Pedogenic iron-oxides ( $Fe_d$ ) were determined by dithionite-citrate-hydrogen carbonate  
234 extraction (Holmgren, 1967). Poorly to non crystallised Fe-oxides ( $Fe_o$ ) were determined by  
235 acid ammonium extraction (Schwertmann (1964). The extractions were analysed at a  
236 wavelength of 238.204 nm by an inductively coupled plasma optical emission spectrometer  
237 (Vista Pro CCD Simultaneous ICP-OES, Varian, USA).

### 238 3.2.3 Ion chromatography

239 The initial water content in the investigated soil material was too low to extract sufficient  
240 amounts of pore water for ion chromatography. Hence, the soil samples were leached, according  
241 to Blume et al. (2011). Five grams of soil material were suspended in 25ml deionized water,  
242 shaken for 90 minutes and centrifuged at 9000rpm to separate the soil material from the soil  
243 solution and sterile filtered through a 0.22 $\mu$ m PES filter (Sartorius AG, Germany).

244 The ion concentrations in leached water samples were analysed by using two ion  
245 chromatography (IC) systems (SYKAM Chromatographie Vertriebs GmbH, Germany). For  
246 cations, the IC system consisted of a 4.6 x 200 mm Reprosil CAT column (Dr. Maisch HPLC  
247 GmbH, Germany), an S5300 sample injector and an S3115 conductivity detector (both SYKAM  
248 Chromatographie Vertriebs GmbH, Germany), 175mg L<sup>-1</sup> 18-Crone-6 and 120 $\mu$ L  
249 methanesulfonic acid served as the eluent with a set flow rate of 1.2mL min<sup>-1</sup>. The injection  
250 volume was 50 $\mu$ L. The column oven temperature was set at 30°C. The Cation Multi-Element  
251 IC-standard (Carl Roth GmbH + Co. KG, Germany) containing  $NH_4^+$ ,  $Ca^{2+}$ ,  $K^+$ ,  $Li^+$ ,  $Mg^{2+}$ ,  $Na^+$   
252 was measured before every replication series. For anions, the IC system consisted of a SeQuant  
253 SAMS anion IC suppressor (Merck KGaA, Germany), an S5200 sample injector, a 3.0 x  
254 150mm Sykrogel A 01 column and an S3115 conductivity detector (all SYKAM  
255 Chromatographie Vertriebs GmbH, Germany). 6mM  $Na_2CO_3$  with 90 $\mu$ M sodium thiocyanate  
256 served as the eluent with a set flow rate of 1 ml min<sup>-1</sup> and a column oven temperature of 50°C.  
257 The injection volume was 50  $\mu$ L. The multi-element anion standard containing  $F^-$ ,  $Cl^-$ ,  $Br^-$ ,  $NO_2^-$ ,  
258  $NO_3^-$ ,  $PO_4^{3-}$  and  $SO_4^{2-}$  was measured before every replication series. The standards and  
259 samples were measured in triplicates.

### 260 3.2.4 Weathering indices and pedogenic oxide ratios

261 The KN Index A ( $(SiO_2+CaO+K_2O+Na_2O)/(Al_2O_3+SiO_2+CaO+K_2O+Na_2O)$ ) was calculated  
262 after Kronberg and Nesbitt (1981). The index is based on the relative enrichment of the Al and  
263 Si oxide phase and the leaching of Na, K and Ca. It ranges between 0 (prevailing chemical  
264 weathering) and 1 (prevailing physical weathering). To get more precise information on the  
265 ongoing chemical weathering, the chemical index of alteration (CIA)  
266  $[(Al_2O_3/(Al_2O_3+Na_2O+CaO^*+K_2O)) \times 100]$  after Nesbitt and Young (1982), in which  $CaO^*$   
267 represents the amount of silicate-bound CaO, was calculated. The CIA is frequently used as a  
268 quantitative measure of feldspar breakdown, assuming that feldspar represents the most



269 abundant and reactive mineral. Higher values indicate increasing weathering intensity.  
270 Additionally, the degree of iron release ( $Fe_d/Fe_t$ ) after Blume and Schwertmann (1969) was  
271 calculated, which gives information on the iron release from primary Fe-bearing mineral  
272 weathering: a longer or more intensive weathering process is indicated by a higher ratio  
273 (Baumann et al., 2014; Mirabella and Carnicelli, 1992).

### 274 3.3 Micromorphology

275 Samples for thin section preparation were air dried and afterwards embedded with a mixture of  
276 resin (Viscovoss N55 S, Vosschemie, Germany), stabilized Styrene (Merck KGaA, Germany)  
277 and hardener (MEKP 505 F, Vosschemie, Germany). After hardening, the samples were  
278 formatted into plane-parallel blocks and halved in the middle using a saw (Woco Top 250 A1,  
279 Uniprec Maschinenbau GmbH, Germany), and then one half was ground with the grinding  
280 machine (MPS-RC Vacuum, G&N GmbH, Germany) and mounted onto a glass carrier. Then  
281 the mounted samples was sawed into slices of about 150 $\mu$ m thickness. Finally, these slices were  
282 ground to a thickness of 25 $\mu$ m. The preparation followed the instructions given by Kühn et al.  
283 (2017). Afterwards, they were analyzed by using a polarizing microscope (ZEISS Axio  
284 Imager.A2m, Software AxioVision 4.7.2, Carl Zeiss Microscopy GmbH, Germany) and  
285 described following the terminology of Stoops (2003).

### 286 3.4 Microbial community analysis

#### 287 3.4.1 Nucleic acids extraction

288

289 For each soil sample (maximum amount of 0.5g per sample), triplicates of total genomic DNA  
290 were extracted using the FastDNA™ Spin Kit for Soil (MO BIO Laboratories Inc., USA). The  
291 extracted DNA was stored at -20°C and used as a template for the enumeration of target genes  
292 by quantitative PCR (qPCR) and next-generation sequencing (Illumina HiSeq).

#### 293 3.4.2 Quantification of bacterial 16S rRNA gene copy numbers

294 qPCR was used to quantify total bacterial abundances. All qPCR assays were performed in  
295 triplicates on a CFX96 Real-time thermal cycler (Bio-Rad Laboratories Inc., CA, USA) and  
296 contained 10 $\mu$ l SensiFAST SYBR Mix (Bioline GmbH, Germany), 5.92 $\mu$ l PCR water, 0.04 $\mu$ l  
297 of forward and reverse primer (100 $\mu$ M) and 4 $\mu$ l template. The quantification of the bacterial  
298 16S rRNA gene was based on the primers 341F (5'-CCTACGGGAGGCAGCAG-3') and 534R  
299 (5'-ATTACCGCGGCTGCTGG-3') according to Muyzer et al., 1993. After an initial  
300 denaturing phase of 3 minutes at 95°C, the cycler included 35 cycles of 3 seconds at 95°C, 20  
301 seconds at 60°C and 60 seconds at 72°C plus the plate read. All cycling programs included a  
302 melting curve from 60°C to 95°C with 0.5°C steps per plate read. The analysis of quantification  
303 data was performed with the CFX Manager™ Software (Bio-Rad Laboratories Inc., CA, USA).



### 304 3.4.3 Illumina HiSeq-Sequencing

305 Unique combinations of tagged 515F (5'-GTGCCAGCMGCCGCGGTAA-3') and 806R (5'-  
306 GGACTACHVGGGTWTCTAAT-3') (Caporaso et al., 2010) primers were assigned to each  
307 sample (Tab. S1, S2). For each sample, two PCR reactions were prepared and the PCR product  
308 pooled after PCR reduce PCR variability. The PCR was performed on a T100™ Thermal Cycler  
309 (Bio-Rad Laboratories Inc., CA, USA) in 25µl reactions, containing 0.125µl OptiTaQ DNA  
310 Polymerase and 2.5 10x Pol Buffer B (Roboklon GmbH, Germany), 1µl MgCl<sub>2</sub> (25mM), 1µl  
311 dNTP Mix (5mM), 16.625µl PCR water, each 0.625µl of forward and reverse primer (20µM)  
312 and 2.5µl genomic DNA. The following cycler program was used: Initial denaturing step for 3  
313 minutes at 95°C followed by 10 cycles of 1 minute at 94°C, 1 minute at 53°C (-0.2°C/cycle)  
314 and 1 minute at 72°C, followed by 20 cycles of 1 minute at 94°C, 1 minute at 50°C and 1 minute  
315 at 72°C, followed by a final extension step for 10 minutes at 72°C. All barcoded samples were  
316 pooled into a single sequencing library by adding an equal amount of DNA (60ng DNA per  
317 sample). Subsequently, a purification of the PCR product pool was achieved by using the  
318 Agencourt AMPure XP – PCR Purification (Beckman Coulter, Inc., CA, USA). The Illumina  
319 HiSeq-sequencing was performed by GATC Biotech AG, Germany.

### 320 3.4.4 Bioinformatics and statistical analysis

321 Sequencing was performed on an Illumina HiSeq (2 x 300 bp). Dual-indexed reads were  
322 demultiplexed using CutAdapt (options: e0.1; trim-n; Martin, 2011). Barcode base pairs were  
323 required to have a phred quality score of Q25 and no mismatches were allowed. Read pairs  
324 were merged using PEAR (options: Q25; p10<sup>-4</sup>; o20; Zhang et al., 2013). The orientation of all  
325 sequences were standardized by an own script using the information from demultiplexing.  
326 Sequences containing low-quality base pairs were trimmed and filtered using Trimmomatic  
327 (quality score of at least Q25 for trailing and leading base pairs, sliding window length of 5  
328 basepairs, minimum sequence length of 200; Bolger et al. 2014). QIIME (version 1.9.1)  
329 (Caporaso et al., 2010) was employed for microbiome analysis. USEARCH 6.1 (Edgar, 2010)  
330 was used for the detection and removal of chimeric sequences. The SILVA database (version  
331 128) (DeSantis et al., 2006) was utilized for the clustering of (OTUs) (97% sequence similarity)  
332 and their taxonomic assignments. Singletons, OTUs assigned to chloroplasts and mitochondria  
333 as well as rare OTUs (relative abundance of <0.1% within each sample) were removed. Sample  
334 triplicates were merged by the mean value of their relative abundance before visualization of  
335 the sequencing data and before analysis of correlating environmental factors. For the processing  
336 and visualization of the obtained OTU table, R and PAST3 (Hammer et al., 2001) were used.  
337 The hierarchical clustering of the samples using the average linkage method was based on the  
338 Bray-Curtis dissimilarity. CANOCO5 (Šmilauer and Lepš, 2014) was used for the canonical  
339 correlation analysis (CCA). If the Bonferroni corrected *p*-value was <0.05, a given  
340 environmental parameter was included. Demultiplexed raw sequencing data were submitted to  
341 the European Nucleotide Archive (<http://www.ebi.ac.uk/ena>) under accession number:  
342 PRJEB29853.



## 343 4 Results

### 344 4.1 Field properties and soil classification

345 Both soils derived from coarse-grained marine sand- and siltstones, which were covered with  
346 volcanic clasts. There was a higher contribution of volcanic material in BB than in SMC.  
347 Neither SMC nor BB showed any ornithogenic influence. Both sites were virtually unvegetated  
348 by cryptogamic or vascular plants. The C-horizon was the only distinct soil horizon occurring at  
349 SMC, whereas BB shows two changes within horizontal structures by abrupt textural change  
350 below 10 cm and 20 cm. The textural change below 20 cm goes along with a change in textural  
351 class; SCL (Sand: 52.5%, Silt: 21.9% and Clay: 25.6%) - CL (Sand: 44%, Silt: 27.2% and Clay:  
352 28.8%). Different from macroscopic features of the soil profiles, both soils showed evidences  
353 of a downward transport and accumulation of particles and nutrients, e.g. soluble products most  
354 likely originating from sea spray (Tab. 1). Accumulation starts at a depth of 50cm at SMC and  
355 below 20cm at BB. Soil color did not change through the profiles. SMC was brown to yellowish  
356 brown and BB was brownish yellow.

357 Formation of platy and lenticular aggregates due to repeated freezing and thawing processes  
358 was detected. Neither platy and lenticular platy structures nor the results of translocation  
359 (eluviation) processes were observed during fieldwork, but could be confirmed later using  
360 micromorphology. Both soils were classified as Cryosols (eutric, loamic) according to the WRB  
361 (IUSS Working Group WRB, 2015).

### 362 4.2 Grain size distribution and soil chemistry

363 SMC had higher sand contents (mean value 61.7%, Table 1), while BB was characterized by  
364 lower sand contents (mean value 47.4%) and higher silt and clay contents (mean values 25.3%  
365 and 27.2% respectively). The grain size distribution varied only slightly with depth and similar  
366 clay and silt contents were demonstrated for both soils.

367 The pH was slightly to moderately alkaline in both profiles and highly alkaline only in the upper  
368 5cm of BB. The pH values followed opposing trends with depth, increasing in SMC from 7.7  
369 to 8.1 and decreasing in BB from 8.6 to 7.4. The EC ranged between 50-60 $\mu\text{S cm}^{-1}$  in SMC and  
370 was substantially higher in BB with a minimum of 350-450 $\mu\text{S cm}^{-1}$  within 5-50cm and its  
371 highest values around 900 $\mu\text{S cm}^{-1}$  between 0-5cm and from 50cm downwards. According to  
372 the EC values, SMC and the middle part of BB can be considered as being salt-free, whereas  
373 the salt content in the upper and lowermost part of BB was low (Food and Agriculture  
374 Organization of the United Nations (FAO), 2006).

375 The total inorganic carbon (TIC) content was low in both soils ranging between 0.01 and 0.03%  
376 in SMC and between 0.07 and 0.2% in BB. This transforms to a TOC content of 0.8-0.9mg g<sup>-1</sup>  
377 at SMC and a TOC content that varied between 1.4 and 2.6mg g<sup>-1</sup> and slightly increased with  
378 depth at BB. The N content was around 0.4mg g<sup>-1</sup> across both soil profiles. The C/N ratio was  
379 generally low with values below 7.5 in both soils, it decreased with depth in SMC (2.6 – 2.1)  
380 and increased with depth in BB (4.0-7.4).



381 Ion concentrations (Tab. 1) were parallel to the depth function of the conductivity in both  
382 soils; e.g. higher EC and ion concentration characterized BB.  $\text{Cl}^-$  concentrations decreased with  
383 depth in SMC from 20.5 to  $3.5\mu\text{mol g}^{-1}$  soil as well as in BB from 4,522 to  $231\mu\text{mol g}^{-1}$  soil.  
384 The highest  $\text{SO}_4^{2-}$  concentrations were observed in the shallow (SMC:  $9.6\mu\text{mol g}^{-1}$  soil; BB:  
385  $621\mu\text{mol g}^{-1}$  soil) and deepest (SMC:  $15.3\mu\text{mol g}^{-1}$  soil; BB:  $451\mu\text{mol g}^{-1}$  soil) samples.  $\text{K}^+$ ,  
386  $\text{Mg}^+$  and  $\text{Ca}^+$  concentrations followed the same trend as  $\text{SO}_4^{2-}$ .  $\text{Br}^-$ ,  $\text{NO}_2^-$ ,  $\text{NO}_3^-$  and  $\text{PO}_4^{3-}$ .  $\text{Li}^+$   
387 and  $\text{NH}_4^+$  concentrations were below the detection limit.

388

389 [ Table 1 ]

390

### 391 4.3 Weathering indices and pedogenic oxide ratios

392 The KN Index A was at 0.91-0.92 in SMC and only slightly lower with 0.89 - 0.90 in BB (Table  
393 2). The CIA varied between 53.9 and 54.8 in SMC and between 56.9 and 58.8 in BB. Both  
394 indices indicated weak chemical weathering with a slightly higher weathering intensity in BB.  
395 Weathering indices were calculated according to the major element contents (Table 3).

396

397 [ Table 2 ]

398 [ Table 3 ]

399

400 The  $\text{Fe}_d/\text{Fe}_t$  ratio showed a decreasing trend from 0.18 to 0.11 with depth in SMC indicating a  
401 decreasing intensity of pedogenic processes with depth. No particular trend was found in BB;  
402 but the  $\text{Fe}_d/\text{Fe}_t$  ratio is – similar to the CIA - generally higher around 0.20 except for 0.16 in the  
403 upper 5cm.

### 404 4.4 Micromorphology

405 SMC had a weak to moderately developed pedality and a weak to moderate degree of separation  
406 (Table 3). Both, pedality and degree of separation are well developed at a depth of 50-60cm  
407 and were lowest developed close to the surface and at the bottom of the profile. In contrast, BB  
408 had a well-developed pedality and a moderate to high degree of separation with its maximum  
409 development close to the bottom of the profile.

410

411 [ Table 4 ]

412

413 Lenticular and subangular blocky microstructures were present in both profiles, whereas  
414 lenticular microstructure was dominant in SMC and subangular blocky microstructure was  
415 dominant in BB. Lenticular shaped aggregates were first observed at a depth of 10cm in profile  
416 BB, and at 30cm in SMC (Figures 6a and 6b).

417

418 [ Figure 6 ]



419

420 Translocations features, like cappings consisting of clay and silt particles welded together with  
421 sand-sized quartz grains were present in the upper part of both profiles. Link cappings occurred  
422 in the lower part of both profiles, with lesser and smaller cappings in BB (Fig. 6d). Link  
423 cappings were very rare and occurred only where coarse rock fragments were located close to  
424 each other. Dusty silt and clay pendants occurred only in the lower part of BB (20-50cm) (Fig.  
425 6e). The sphericity of mineral grains was smooth in both profiles. The minerals were slightly  
426 better rounded in BB (subangular to round) than in SMC (subangular to subrounded).  
427 Weathering processes were identified by pellicular and dotted alteration patterns on rock  
428 fragments (mostly in sandstone fragments) in both profiles with a higher number of fragments  
429 with dotted alteration patterns than with pellicular alteration patterns. The quantity and intensity  
430 of dotted alteration patterns decreased with depth. Larger rock fragments were often strongly  
431 weathered, so that mainly quartz-minerals were still preserved (Figure 6f). Besides quartz,  
432 glauconite is the main mineral component in the unweathered sandstone fragments. In addition,  
433 feldspars and micas occur to a very small extent. The sandstones cemented by fine material and  
434 faint Fe coatings are visible around quartz grains. Pellicular alteration pattern was found  
435 exclusively on volcanic rock fragments, and only in the uppermost thin section (0-10cm) of  
436 SMC (Figure 6g). Fragments showing pellicular alteration patterns occurred in 10-30cm of BB.  
437 Even though the number of weathered fragments decreased, pellicular patterns were slightly  
438 thicker in slide BBII (20-30cm) than in BBI (10-20cm). However, pellicular alteration patterns  
439 did not exceed the state of “pellicular” in any analyzed slide whereas dotted alteration patterns  
440 often reach the state of “patchy cavernous residue” (Figure 6e) and do occur also as dispersed  
441 minute residues (Stoops, 2003).

#### 442 **4.5 Microbial abundance and community structure**

443 The enumeration of the 16S rRNA gene revealed a similar trend for both soil profiles (Fig. 7).  
444 The highest abundances with  $6.6 \times 10^8$  copies  $g^{-1}$  soil (BB) and  $1.7 \times 10^8$  copies  $g^{-1}$  soil (SMC)  
445 were detected in the uppermost depth increment of both soil profiles. Both soils showed a  
446 decrease in bacterial abundances with depth. The lowest bacterial abundances in SMC were  
447 detected below 50cm depth with  $3.7 \times 10^5$  copies  $g^{-1}$  soil, and in BB in 20-50cm depth with  $1.7$   
448  $\times 10^6$  copies  $g^{-1}$  soil.

449 In total, 19,759,767 reads were obtained after merging the forward and reverse reads,  
450 demultiplexing, filtering and deletion of chimeric sequences. Additionally, reads of singletons,  
451 chloroplast/mitochondria-associated OTUs as well as rare OTUs were filtered, resulting in  
452 15,407,464 reads. The number of reads per sample ranged from 54,122 to 916,583 with a mean  
453 value of 513,582. A total of 687 OTUs was clustered. After taxonomic classification, 258  
454 putative taxa were obtained. Shannon's H index was used to estimate and compare the alpha  
455 diversity of the different depth increments interval of the soils (Tab. S3). Both soils showed a  
456 similar Shannon's H index, which ranged from 3.7 to 4.7 not following any specific trend.

457 Bacteria dominated the microbial community in both soil profiles (Fig. 7). Higher abundances  
458 of Thaumarchaeota (7.2 - 12.9%) were found in the upper 10cm of the soil profile from SMC



459 (Tab. S4). On a phylum level, the soil profile of SMC was dominated by Proteobacteria (23.4 -  
460 57.9%) and Actinobacteria (17.7–41.3%) but showed also relative high abundances of  
461 Acidobacteria (3.9-14.1%). The microbial community in BB was also mainly composed of  
462 Proteobacteria (28.2-30.8%), followed by Actinobacteria (27.6-46.6%), Gemmatimonadetes  
463 (3.9-24.7%) and Chloroflexi (5.3-10.9%). Bacteroidetes were highly abundant (10.5%) in the  
464 top 5 cm of BB.

465

#### 466 [ Figure 7 ]

467

468 The distribution of dominant OTUs was reflected by a cluster analysis based on the Bray-Curtis  
469 dissimilarity of the investigated depth increments. Samples were clustered according to their  
470 origin and depth. On a first level, samples grouped according to depth in upper (0–20cm) and  
471 deeper (20-80cm) samples and within these groups they clustered according to location (BB vs.  
472 SMC). An exception is the sample from BB from the depths 0–5cm which formed an own  
473 cluster (Fig. 8). The deeper samples in both profiles (20–80cm depth) showed high relative  
474 abundances of three OTUs related to Acidiferrobacteraceae(1, 2, 3) (SMC: 1.7-14.6%; BB: 2.2-  
475 9.8%) and one OTU related to Gemmatimonadaceae(1) (SMC: 1.5-3.8%; BB: 14.1-20.3%).  
476 High proportions of two OTUs related to Gammaproteobacteria(1, 2) (SMC: 2.8-11.4%; BB:  
477 5.4-10.2%) and one OTU related to Gaiellales(2) (SMC: 3.7-5.7%; BB: 7.2-8.3%) were  
478 observed in the shallow samples (0-20 cm). BB 0-5 cm was comprised of a strongly different  
479 community. The most abundant taxa in this sample were related to *Thermomonas*(1) (6.4%),  
480 *Sphingomonas* (3.7%) and *Solirubrobacterales*(1) (3.7%).

481

#### 482 [ Figure 8 ]

483

484 The relationship of OTU distribution and environmental parameters was examined by applying  
485 a CCA (Fig. 9). Contents of chloride (18.5%), calcium (11.8%), sulfate (5.9%), silt (5.6%),  
486 TOC (6%) and the Fe<sub>d</sub>/Fe<sub>t</sub>-ratio (12.5%) formed the optimal subset to explain variations in  
487 community structure of the investigated soil profiles ( $p < 0.05$ ). The adjusted explained  
488 compositional variation was 49.9%. A strong correlation between the unique community of BB  
489 0-5cm and the saline conditions was observed, mainly caused by high sulfate and chloride  
490 concentrations. The remaining samples were arranged according to sample site and depth as  
491 already observed in the cluster analysis above.

492

#### 493 [ Figure 9 ]

494 **5 Discussion**

495 The interaction of biotic and abiotic processes remains one of the fundamental questions in  
496 ecosystem research and further the initial development of soils under harsh environmental  
497 conditions, such as Antarctica. So far, only a few studies exist for polar environments that  
498 integrate pedogenic and microbiological research (e.g. Aislabie et al. 2008, Cowan et al. 2014,  
499 Ganzert et al. 2011; Bajerski and Wagner, 2013). Due to the absence of vascular plants, the ice-  
500 free area of JRI is a pristine laboratory and offers the exceptional opportunity to improve our  
501 understanding of the interrelations between soil formation and microbiological properties. The  
502 present interdisciplinary study gives profound insights in the state of soil formation and  
503 microbial community structure in initial soils in the transition zone between maritime and  
504 continental Antarctica.

505 James Ross Islands is located in the transition zone between warmer and wetter maritime  
506 Antarctica and cold and dry continental Antarctica (Souza et al., 2014). In this area, we studied  
507 two representative soils 16km apart, with different exposures to the dominant south-westerly  
508 winds. The leeward position of SMC displays formation conditions of a typical inland soil,  
509 while BB in its windward position represents coastal soils. As indicated by EC values, BB is  
510 influenced by sea spray, while SMC, sheltered behind the Lachman Crags, does not show strong  
511 input of soluble salts from sea spray.

512 The examined soils on JRI were characterized by low TOC (0.09%-0.26%) and low total  
513 nitrogen contents (approx. 0.04%), which is common for Antarctic soil environments (e.g.  
514 Cannone et al., 2008), and relative high pH values (7.4- 8.6). The moderately to highly alkaline  
515 pH in both soils cannot be explained by the occurrence of CaCO<sub>3</sub>, because the soils have a  
516 negligible amount with  $\leq 0.2$  %. Low C and P contents do not only show the missing influence  
517 of penguins, but also indicate a relative juvenility of the soils: This indicates that no cations  
518 have been leached from the topsoil, and therefore the pH remains neutral to basic (Wilhelm et  
519 al., 2016). In addition, the content of basalt clasts in the parent material results in increased soil  
520 pH values (Simas et al., 2002; Moura et al., 2012). The opposing trends in the depth function  
521 of the pH values are caused by the input of soluble salts from sea spray: wind can transport  
522 soluble salts from the sea causing an additional input of bases simultaneously increasing the pH  
523 at BB, while SMC is not affected (Benassai et al., 2005; Russell et al., 2010; Hara et al., 2004;  
524 Udisti et al., 2012). Since the substrate was not colonized by plants, lichens or endolithic  
525 prokaryotes, and the taxonomic data revealed low abundances of phototrophic organisms, the  
526 alkalization of the substrate by the release of hydroxyl ions in the course of photosynthesis has  
527 a minor effect on soil pH. On the other hand, the neutral to basic pH does not significantly affect



528 the soil microbial community structure, which is in accordance with observations in soils from  
529 Livingston Island (South Shetland Archipelago, maritime Antarctica) by Ganzert et al. (2011).  
530 They explained it by the occurrence of a specific soil microbial community, which thrives under  
531 low C and N conditions and is not depending on nutrient input. Therefore, pH is mainly driven  
532 by the parent material composition combined with the input of soluble salts in these young soils  
533 on JRI.

534 The additional input of airborne cations by sea spray led to higher sodium and calcium contents  
535 and a rejuvenation of the affected depth increments of the soil profile, which can be seen in the  
536 lower CIA values in 0-5 cm soil depth of both soils compared to the lower part of the profiles.  
537 Ions, for instance sulfate accumulate close to the permafrost table, which acts as a barrier and  
538 therefore explains increasing contents of sulfate with depth. The high amount of sulfate near  
539 the surface is most likely caused by sea spray and precipitation, because they are known to carry  
540 high amounts of sulfate in coastal areas (Blume et al., 2010).

541 Chemical weathering, as indicated by the KN-Index A (Kronberg and Nesbitt, 1981), is only of  
542 minor importance whereas physical weathering is prevailing. The CIA and pedogenic oxide  
543 ratios (POR) confirmed the low degree of soil formation. Pedogenic oxides with specific  
544 degrees of crystallization relate to intensity and/or duration of pedogenic processes (Baumann  
545 et al., 2014; Blume and Schwertmann, 1969; Mirabella and Carnicelli, 1992). The results show  
546 that both CIA and both POR are slightly higher at BB compared to SMC. The KN-Index A and  
547 the CIA showed a weak chemical weathering of these mineral soils (Michel et al., 2014). Both  
548 indices indicated a more intensive chemical weathering at BB and, thus, indicate a slightly  
549 stronger pedogenesis at BB than at SMC. This finding could be explained by the sea- and  
550 windward position of BB, which results in an increased water availability and a slightly more  
551 levelled microclimate. Since both soils are located in similar topographic positions and derived  
552 from similar parent material, CIA and POR results allow the interpretation that soils influenced  
553 by coastal conditions tend to be more weathered. Besides physical and chemical weathering,  
554 microorganisms play an important role in mineral dissolution and oxidation. Adapted  
555 microorganisms colonize minerals and are, depending on nutritional requirements, nutrient  
556 availability and mineral type, potential contributors to the weathering of minerals (Uroz et al.,  
557 2009). Taxonomical groups, which are usually connected to microbial weathering, are present  
558 in the soils, such as *Massilia*, *Bacillus* (Ma et al., 2011) and *Polaromonas* (Frey et al., 2010).  
559 Interestingly, the relative abundances of these taxa were lower in the more weathered soil from  
560 BB, which indicates a possible interrelation between the occurrence of these potential  
561 weathering-related organisms and the degree of weathering.



562 Evaluating weathering using the CIA, it must be noted that the value for BB is most likely  
563 underestimated. BB is highly influenced by salts from sea spray, which is known to carry high  
564 amounts of Na (Udisti et al., 2012). The calculation of the CIA takes Na-content into account  
565 (Nesbitt & Young, 1982), and therefore the CIA values would be significantly higher if the  
566 additional input of sea salts could be excluded. It is very likely that the actual difference in state  
567 of weathering between SMC and BB would be much higher. In conclusion, chemical  
568 weathering, even without influence of guano deposits, is of higher importance for the current  
569 state of soil formation, than the ongoing cryoturbation.

570 In case of the pedogenic oxide ratios, a correlation between the microbial community structure  
571 and weathering could be observed, although both soils are at a very initial stage of soil  
572 formation. The pedogenic oxide ratios correlate with the compositional distribution of  
573 microorganisms in the investigated soils, and with the relative abundances of one  
574 Acidiferrobacteraceae-related OTU. Microorganisms of this family are described as autotrophic  
575 sulfur and iron oxidizers, which have the capacity to use ferrous iron, thiosulfate, tetrathionate,  
576 sulfide and elemental sulfur as electron donors and oxygen or ferric iron as terminal electron  
577 acceptor (Hallberg et al., 2011). The reactive iron could potentially be used as terminal electron  
578 acceptor in the course of microbial iron cycling (Canfield, 1989). Organic matter, a potential  
579 substrate for heterotrophic microbial processes, sorbs on mineral surfaces (Kaiser and  
580 Guggenberger, 2000) and could be released in the course microbial oxidation and reduction of  
581 reactive iron phases. In addition to the autotrophic processes, the release of sorbed, organic  
582 matter from mineral surfaces could be an additional way to increase the pool of biologically  
583 available carbon. The availability of such a mechanism potentially has an influence on the  
584 microbial community structure and abundances in oligotrophic environments.

585 Translocation features are common features in permafrost-affected soils. They often occur  
586 together with platy rectangular or lenticular aggregates, caused by reoccurring freeze-thaw-  
587 cycles (Van Vliet-Lanoë, 1985). Platy blocks and lenses dominated the microstructure in the  
588 areas between 20 and 50cm of both profiles. They were absent near the surface of both profiles  
589 and at the bottom of the profile SMC. These microstructures are known to occur in the transition  
590 zone between permanently frozen and unfrozen soils (Shur et al., 2005; Van Vliet-Lanoë et al.,  
591 2004). Here, the alternating temperature and soil moisture conditions additionally affect the  
592 microbial community structure. The frequency of freeze-and-thaw cycles tends to be steady in  
593 the middle part of a permafrost-affected soil, whereas weather shifts influence the surface,  
594 causing several freeze-and-thaw events per day, which do not result in typical microstructure  
595 formation due to insufficient water supply (Van Vliet-Lanoë, 1985). Aggregate formation by



596 reoccurring freeze-and-thaw cycles result in a change in pore shape and size (Van Vliet-Lanoë  
597 et al., 2004). Especially during the summer season, intensive insolation causes high evaporation,  
598 resulting in dry soil surfaces. Changes in pore space affects microbial habitats, due to larger  
599 pores and a more sufficient water supply. This has a severe influence on matter fluxes and soil-  
600 environmental conditions, which is reflected in a changing species distribution and, more  
601 specifically, the occurrence of different clusters of highly abundant organisms in both soils.  
602 Nevertheless, freeze-and-thaw cycles definitely also occur in the upper part of the profile, as  
603 indicated by the well sorted areas (Van Vliet-Lanoë, 1985), which were described as single  
604 grain microstructure. Near the permafrost table aggregates are often formed by frost desiccation  
605 and are hence poorly compacted what makes them unstable upon moistening, which occurs  
606 during thawing events and explains the missing platy microstructure at SMC near the bottom  
607 of the profile (Van Vliet-Lanoë, 2010). The fact that lenticular shaped aggregates occur also in  
608 the lower part of the profile indicates that the permafrost table is located underneath the layer  
609 of coarse gravel at BB.

610 Although the investigated soils were poorly developed, an abundant and diverse prokaryotic  
611 community could be observed. Microbial abundances in both soils showed a decreasing trend  
612 with depth. Values of up to  $10^9$  gene copies  $g^{-1}$  soil in the uppermost depth increments are  
613 comparable to observed microbial abundances from other cold environments, such as alpine  
614 glacial forelands (Sigler et al., 2002), permafrost-affected soils from arctic regions (Liebner et  
615 al., 2008) and Antarctic glacier forefields (Bajerski and Wagner, 2013).

616 Both soils were characterized by a highly diverse community dominated by Proteobacteria,  
617 Actinobacteria, Gemmatimonadetes, Acidobacteria and Chloroflexi, which is in accordance  
618 with the observations in other continental and maritime Antarctic habitats (e.g. Yergeau et al.,  
619 2007; Cary et al., 2010, Ganzert et al., 2011, Bajerski and Wagner 2013, Wang et al., 2016).  
620 Substantial differences in geochemical parameters such as conductivity, the change of the  
621 community structure on a phylum level were evident as well as the occurrence of depth-  
622 dependent clusters (0-20 cm; >20 cm) of dominant OTUs (Fig. 8). Whereas the upper 20cm of  
623 the soils were dominated by Gammaproteobacteria and Gaiellales, the deeper part of the soils  
624 showed increased abundances of OTUs related to Acidiferrobacteraceae and  
625 Gemmatimonadaceae. This distinct shift correlates with the occurrence of the microstructure  
626 related to freezing and thawing and could be related to its changes of the pore space and the  
627 availability of oxygen, water and nutrients. For instance, Gemmatimonadaceae were a common  
628 observation in the soils and showed increased abundances in deeper parts of BB. These  
629 organisms have a cosmopolitan distribution in terrestrial environments and depend on the soil



630 moisture condition of the respective soil and soil depth (DeBruyn et al., 2011; Bajerski and  
631 Wagner, 2013). Only a few isolates have been described for this phylum (e.g. Zeng et al., 2015)  
632 and their exact functions in soil ecosystems remain uncertain. The change in relative abundance  
633 of these taxa with depth could be coupled to the changing availability of water, which depends  
634 on the microstructure. Thus, in addition to environmental parameters, which shape the overall  
635 prokaryotic community, the microstructure of the initial soils has a substantial influence on  
636 species distribution.

637 Higher abundances of Bacteroidetes- and especially Flavobacteriaceae-related OTUs were  
638 observed in the uppermost area of soil from BB, while only showing minor abundances in the  
639 deeper soil areas. This area differed from the remaining soil in two regards, namely very high  
640 chloride concentrations and a relative high content of coarse sandy material and could select  
641 for adapted psychro- and halotolerant Bacteroidetes-related organisms, such as  
642 Flavobacteriaceae (e.g. Bajerski et al., 2013a). Members of the Flavobacteriaceae family  
643 detected in this area, for instance *Gillisia sp.*, were isolated from Antarctic habitats before and  
644 were shown to be at least moderately tolerant to saline conditions (Bowman and Nichols, 2005).  
645 Putative halotolerant or halophilic Flavobacteriaceae in this area could have a need for high  
646 chloride contents. Chloride can be accumulated inside the cell to osmotically balance the  
647 cytoplasm with the surrounding habitat (Oren et al., 2002; Müller and Oren, 2003).  
648 Furthermore, the detected Bacteroidetes-related organisms could prefer the coarser, sandy  
649 microstructure from this depth increment. The preference of microbial groups for certain grain-  
650 size-dependent microenvironments, for instance the sand-sized fraction being preferred by  
651 Bacteroidetes, was shown, e.g. in Typic Hapludalfs from central Denmark (Hemkemeyer et al.,  
652 2018).

653 Both investigated soils were poor in soil organic C as well as N. Organisms with the ability to  
654 use oxygenic photosynthesis to fixate CO<sub>2</sub>, such as cyanobacteria, were nearly absent in the  
655 investigated soils. Several of the most abundant taxa observed in BB and SMC were putative  
656 chemoautotrophs involved in nitrogen, iron and sulfur cycling, such as potential ammonia-  
657 oxidizing Thaumarchaeota or sulfur/iron-oxidizing Acidiferrobacteraceae. Microorganisms can  
658 be seen as the primary pioneers of nutrient-poor environments such as Antarctic soils, and were  
659 shown to have the genetic potential to fixate C and N (Cowan et al., 2011; Niederberger et al.,  
660 2015), thus increasing C and N contents of these oligotrophic soils. The chemoautotrophic  
661 Thaumarchaeota oxidize ammonia aerobically to nitrite (Brochier-Armanet et al., 2008; Vajrala  
662 et al., 2013) and were observed in many studies located in Antarctica (Magalhães et al., 2014;  
663 Ayton et al., 2010). These organisms are reported to have the genetic potential to use the



664 hydroxypropionate/hydroxybutyrate pathway for CO<sub>2</sub> fixation, which is highly efficient and  
665 could provide an ecological advantage in oligotrophic environments (Könneke et al., 2014).  
666 Additionally, OTUs related to the phylum Actinobacteria and the associated orders  
667 Acidimicrobiales and Solirubrobacterales were highly abundant. Microorganisms in Antarctic  
668 soils, especially bacteria related to the phyla Actinobacteria, AD3 and WPS-2, were shown to  
669 generate biomass by consuming H<sub>2</sub>, CO<sub>2</sub> and CO from the atmosphere (Ji et al., 2017). The  
670 gene for chemosynthetic CO<sub>2</sub> fixation, *rbcLIE*, was found in multiple orders, including  
671 Pseudonocardiales, Acidimicrobiales and Solirubrobacterales. Similar functional capabilities  
672 could be present and active in the investigated soils. Our results show that, in this initial stage  
673 of soil development, chemolithoautotrophic lifestyles plays an important role for the generation  
674 of biomass and initial accumulation of soil organic carbon and nitrogen.

## 675 6. Conclusion

676 The presented soil and microbiological study on initial soils in the semiarid environment of  
677 Antarctica shows the current state of soil formation indicated by main soil and microbiological  
678 properties and their interplay. The results allow us to draw the following conclusions:

- 679 1. Despite similarities in topographic position and substrates, both profiles showed distinct  
680 differences in chemistry (content of salts indicated by EC, opposing trends in pH and  
681 states of weathering, indicated by WI and POR) and microbiology (depth functions of  
682 microbial abundances and diversity, e.g. Proteobacteria, Gemmatimonadetes and  
683 Thaumarchaeota abundances), which are caused by the different local environmental  
684 conditions prevailing at both sites.
- 685 2. The EC values as well as the depth function of the pH values clearly showed different  
686 conditions for soil formation at the two sites due to the more exposed towards the mainly  
687 south-westerly winds location of BB, resulting there in a more intense weathering and  
688 soil formation.
- 689 3. Taking weathering and aggregation as indicators of soil formation, we conclude that  
690 coastal conditions - in contrast to inland conditions - favor the formation of soils in  
691 maritime Antarctica.
- 692 4. Despite the different predominant climatic conditions of soil formation, the microbial  
693 communities differ more distinctly between the depth increments in one profile than  
694 between the two profiles. Therefore, we conclude that in this initial stage of soil  
695 formation factors such as weathering and microstructure formation, as well as the



696 resulting parameters (e.g. water availability and matter fluxes), are of greater importance  
697 than chemical parameters such as EC and pH.

698 5. Assuming that prokaryotic life is highly affected by changes in soil structure and vice  
699 versa, further investigations in this field should include analyses of (micro-) aggregates.

700

701 *Author Contributions.* The project was initiated and designed by Dirk Wagner, Peter Kühn,  
702 Thomas Scholten and Carsten W. Mueller. Lars A. Meier and Carsten W. Mueller carried out  
703 fieldwork during the PROANTAR fieldtrip led by Carlos E.G.R. Schaefer in 2016. Lars A.  
704 Meier, Patryk Krauze, Isabel Prater and Fabian Horn did analyses and interpretation. Lars A.  
705 Meier and Patryk Krauze prepared this manuscript with contributions from all co-authors.

706

707 *Competing interests.* The authors declare that they have no conflict of interests.

708

709 *Acknowledgements.* We thank the Brazilian Navy and the Brazilian Antarctic Expedition  
710 PROANTAR for all logistics and help in the field during southern summer 2015/2016. We  
711 especially acknowledge the supported by the German Research Foundation (DFG) in the  
712 framework of the priority programme 1158 ‘Antarctic Research with Comparative  
713 Investigations in Arctic Ice Areas’ by a grant to DW (WA 1554/18), TS (SCHO 739/18), PK  
714 (KU 1946/8) and CWM (MU 3021/8).

## 715 References

716 **Aislabie, J. M., Jordan, S., and Barker, G. M.:** Relation between Soil Classification and Bacterial Diversity in  
717 Soils of the Ross Sea Region, Antarctica, *Geoderma*, 144, 9-20,  
718 <http://dx.doi.org/10.1016/j.geoderma.2007.10.006>, 2008.

719 **Ayton, J., Aislabie, J., Barker, G., Saul, D., and Turner, S.:** Crenarchaeota Affiliated with Group 1.1 B Are  
720 Prevalent in Coastal Mineral Soils of the Ross Sea Region of Antarctica, *Environmental microbiology*,  
721 12, 689-703, 2010.

722 **Bajerski, F., Ganzert, L., Mangelsdorf, K., Padur, L., Lipski, A., and Wagner, D.:** *Chryseobacterium*  
723 *Frigidisoli* Sp. Nov., a Psychrotolerant Species of the Family Flavobacteriaceae Isolated from Sandy  
724 Permafrost from a Glacier Forefield, *International journal of systematic and evolutionary microbiology*,  
725 63, 2666-2671, 2013.

726 **Bajerski, F., and Wagner, D.:** Bacterial Succession in Antarctic Soils of Two Glacier Forefields on Larsemann  
727 Hills, East Antarctica, *FEMS Microbiology Ecology*, 85, 128-142, 10.1111/1574-6941.12105, 2013.

728 **Balks, M. R., López-Martínez, J., Goryachkin, S. V., Mergelov, N. S., Schaefer, C. E., Simas, F. N., Almond,**  
729 **P. C., Claridge, G. G., Mcleod, M., and Scarrow, J.:** Windows on Antarctic Soil–Landscape  
730 Relationships: Comparison across Selected Regions of Antarctica, *Geological Society, London, Special*  
731 *Publications*, 381, 397-410, 2013.

732 **Baumann, F., Schmidt, K., Dörfer, C., He, J.-S., Scholten, T., and Kühn, P.:** Pedogenesis, Permafrost,  
733 Substrate and Topography: Plot and Landscape Scale Interrelations of Weathering Processes on the



- 734 Central-Eastern Tibetan Plateau, Geoderma, 226–227, 300–316,  
735 <http://dx.doi.org/10.1016/j.geoderma.2014.02.019>, 2014.
- 736 **Benassai, S., Becagli, S., Gragnani, R., Magand, O., Proposito, M., Fattori, I., Traversi, R., and Udisti, R.:**  
737 Sea-Spray Deposition in Antarctic Coastal and Plateau Areas from Itase Traverses, *Annals of Glaciology*,  
738 41, 32–40, 2005.
- 739 **Blume, H.-P., Brümmner, G. W., Horn, R., Kandeler, E., Kögel-Knabner, I., Kretzschmar, R., Stahr, K.,**  
740 **Wilke, B.-M., Thiele-Bruhn, S., and Welp, G.:** Lehrbuch Der Bodenkunde 16. Auflage, edited by:  
741 Scheffer, F., and Schachtschabel, B., Spektrum Akademischer Verlag, Heidelberg, 2010.
- 742 **Blume, H.-P., Chen, J., Kalk, E., and Kuhn, D.:** Mineralogy and Weathering of Antarctic Cryosols, in: *Cryosols*,  
743 Springer, 427–445, 2004.
- 744 **Blume, H.-P., Stahr, K., and Leinweber, P.:** Bodenkundliches Praktikum: Eine Einführung in Pedologisches  
745 Arbeiten Für Ökologen, Land-Und Forstwirte, Geo-Und Umweltwissenschaftler, Springer-Verlag, 2011.
- 746 **Blume, H., and Schwertmann, U.:** Genetic Evaluation of Profile Distribution of Aluminum, Iron, and Manganese  
747 Oxides, *Soil Science Society of America Journal*, 33, 438–444, 1969.
- 748 **Bockheim, J.:** Properties and Classification of Cold Desert Soils from Antarctica, *Soil Science Society of America*  
749 *Journal*, 61, 224–231, 1997.
- 750 **Bockheim, J., Vieira, G., Ramos, M., López-Martínez, J., Serrano, E., Guglielmin, M., Wilhelm, K., and**  
751 **Nieuwendam, A.:** Climate Warming and Permafrost Dynamics in the Antarctic Peninsula Region, *Global*  
752 *and Planetary Change*, 100, 215–223, <http://dx.doi.org/10.1016/j.gloplacha.2012.10.018>, 2013.
- 753 **Bockheim, J. G., Lupachev, A. V., Blume, H. P., Bölter, M., Simas, F. N. B., and McLeod, M.:** Distribution  
754 of Soil Taxa in Antarctica: A Preliminary Analysis, *Geoderma*, 245–246, 104–111,  
755 <https://doi.org/10.1016/j.geoderma.2015.01.017>, 2015.
- 756 **Bolger, A. M., Lohse, M., and Usadel, B.:** Trimmomatic: A Flexible Trimmer for Illumina Sequence Data,  
757 *Bioinformatics*, 30, 2114–2120, 10.1093/bioinformatics/btu170, 2014.
- 758 **Borzotta, E., and Trombotto, D.:** Correlation between Frozen Ground Thickness Measured in Antarctica and  
759 Permafrost Thickness Estimated on the Basis of the Heat Flow Obtained from Magnetotelluric Soundings,  
760 *Cold Regions Science and Technology*, 40, 81–96, <http://dx.doi.org/10.1016/j.coldregions.2004.06.002>,  
761 2004.
- 762 **Bowman, J. P., and Nichols, D. S.:** Novel Members of the Family Flavobacteriaceae from Antarctic Maritime  
763 Habitats Including *Subsaximicrobium Wynnwilliamsii* Gen. Nov., Sp. Nov., *Subsaximicrobium*  
764 *Saxinquilinus* Sp. Nov., *Subsaxibacter Broadyi* Gen. Nov., Sp. Nov., *Lacinutrix Copepodicola* Gen. Nov.,  
765 Sp. Nov., and Novel Species of the Genera *Bizionia*, *Gelidibacter* and *Gillisia*, *International journal of*  
766 *systematic evolutionary microbiology*, 55, 1471–1486, 2005.
- 767 **Brochier-Armanet, C., Boussau, B., Gribaldo, S., and Forterre, P.:** Mesophilic Crenarchaeota: Proposal for a  
768 Third Archaeal Phylum, the Thaumarchaeota, *Nature Reviews Microbiology*, 6, 245, 2008.
- 769 **Cannone, N., Wagner, D., Hubberten, H. W., and Guglielmin, M.:** Biotic and Abiotic Factors Influencing Soil  
770 Properties across a Latitudinal Gradient in Victoria Land, Antarctica, *Geoderma*, 144, 50–65,  
771 <https://doi.org/10.1016/j.geoderma.2007.10.008>, 2008.
- 772 **Canfield, D. E.:** Reactive Iron in Marine Sediments, *Geochimica et Cosmochimica Acta*, 53, 619–632, 1989.



- 773 **Caporaso, J. G., Kuczynski, J., Stombaugh, J., Bittinger, K., Bushman, F. D., Costello, E. K., Fierer, N.,**  
774 **Pena, A. G., Goodrich, J. K., and Gordon, J. I.:** Qiime Allows Analysis of High-Throughput  
775 Community Sequencing Data, *Nature methods*, 7, 335, 2010.
- 776 **Cary, S. C., McDonald, I. R., Barrett, J. E., and Cowan, D. A.:** On the Rocks: The Microbiology of Antarctic  
777 Dry Valley Soils, *Nature Reviews Microbiology*, 8, 129, 2010.
- 778 **Chong, C.-W., Pearce, D. A., and Convey, P.:** Emerging Spatial Patterns in Antarctic Prokaryotes, *Frontiers in*  
779 *microbiology*, 6, 1058, 2015.
- 780 **Chong, C. W., Pearce, D. A., Convey, P., Tan, G. A., Wong, R. C., and Tan, I. K.:** High Levels of Spatial  
781 Heterogeneity in the Biodiversity of Soil Prokaryotes on Signy Island, Antarctica, *Soil Biology and*  
782 *Biochemistry*, 42, 601-610, 2010.
- 783 **Chong, C. W., Pearce, D., Convey, P., Yew, W. C., and Tan, I.:** Patterns in the Distribution of Soil Bacterial  
784 16s Rna Gene Sequences from Different Regions of Antarctica, *Geoderma*, 181, 45-55, 2012.
- 785 **Cowan, D. A., Makhalanya, T. P., Dennis, P. G., and Hopkins, D. W.:** Microbial Ecology and  
786 Biogeochemistry of Continental Antarctic Soils, *Frontiers in Microbiology*, 5, 154,  
787 [10.3389/fmicb.2014.00154](https://doi.org/10.3389/fmicb.2014.00154), 2014.
- 788 **Cowan, D. A., Sohm, J. A., Makhalanya, T. P., Capone, D. G., Green, T. G. A., Cary, S. C., and Tuffin, I.**  
789 **M.:** Hypolithic Communities: Important Nitrogen Sources in Antarctic Desert Soils, 3, 581-586,  
790 [doi:10.1111/j.1758-2229.2011.00266.x](https://doi.org/10.1111/j.1758-2229.2011.00266.x), 2011.
- 791 **Daher, M., Schaefer, C.E.G.R., Fernandes Filho, E.I., Francelino, M.R., Senra, E.O.:** Semi-arid soils from a  
792 topolithosequence at James Ross Island, Weddell Sea region, Antarctica: Chemistry, mineralogy, genesis  
793 and classification, *Geomorphology*, <https://doi.org/10.1016/j.geomorph.2018.11.003>, 2018.
- 794 **Davies, B. J., Glasser, N. F., Carrivick, J. L., Hambrey, M. J., Smellie, J. L., and Nývlt, D.:** Landscape  
795 Evolution and Ice-Sheet Behaviour in a Semi-Arid Polar Environment: James Ross Island, Ne Antarctic  
796 Peninsula, Geological Society, London, Special Publications, 381, 353-395, 2013.
- 797 **DeBruyn, J. M., Nixon, L. T., Fawaz, M. N., Johnson, A. M., and Radosevich, M.:** Global Biogeography and  
798 Quantitative Seasonal Dynamics of Gemmatimonadetes in Soil, *Applied environmental microbiology*,  
799 *AEM*. 05005-05011, 2011.
- 800 **DeSantis, T. Z., Hugenholtz, P., Larsen, N., Rojas, M., Brodie, E. L., Keller, K., Huber, T., Dalevi, D., Hu,**  
801 **P., and Andersen, G. L.:** Greengenes, a Chimera-Checked 16s Rna Gene Database and Workbench  
802 Compatible with Arb, *Applied and environmental microbiology*, 72, 5069-5072, 2006.
- 803 **Edgar, R. C.:** Search and Clustering Orders of Magnitude Faster Than Blast, *Bioinformatics*, 26, 2460-2461,  
804 2010.
- 805 **Engel, Z., Nývlt, D., and Láška, K.:** Ice Thickness, Bed Topography and Glacier Volume Changes on James  
806 Ross Island, Antarctic Peninsula, *Journal of Glaciology*, 58, 904-914, 2012.
- 807 **Food and Agriculture Organization of the United Nations (FAO):** Fao Guidelines for Soil Description, 4th Ed.,  
808 edited by: Food and Agriculture Organization of the United Nations, Rome, 2006.
- 809 **Frey, B., Rieder, S. R., Brunner, I., Plötze, M., Koetzsch, S., Lapanje, A., Brandl, H., Furrer, G. J. A., and**  
810 **microbiology, e.:** Weathering-Associated Bacteria from the Damma Glacier Forefield: Physiological  
811 Capabilities and Impact on Granite Dissolution, 76, 4788-4796, 2010.
- 812 **Ganzert, L., Lipski, A., Hubberten, H.-W., and Wagner, D.:** The Impact of Different Soil Parameters on the  
813 Community Structure of Dominant Bacteria from Nine Different Soils Located on Livingston Island,



- 814 South Shetland Archipelago, Antarctica, *FEMS Microbiology Ecology*, 76, 476-491, 10.1111/j.1574-  
815 6941.2011.01068.x M4 - Citavi, 2011.
- 816 **Hallberg, K. B., Hedrich, S., and Johnson, D. B.:** Acidiferrobacter Thiooxydans, Gen. Nov. Sp. Nov.; an  
817 Acidophilic, Thermo-Tolerant, Facultatively Anaerobic Iron-and Sulfur-Oxidizer of the Family  
818 Ectothiorhodospiraceae, *Extremophiles*, 15, 271-279, 2011.
- 819 **Hammer, Ø., Harper, D., and Ryan, P.:** Past: Paleontological Statistics Software Package for Education and  
820 Data Analysis *Palaeontol. Electronica* 4: 1–9. 2001.
- 821 **Hara, K., Osada, K., Kido, M., Hayashi, M., Matsunaga, K., Iwasaka, Y., Yamanouchi, T., Hashida, G., and  
822 Fukatsu, T.:** Chemistry of Sea-Salt Particles and Inorganic Halogen Species in Antarctic Regions:  
823 Compositional Differences between Coastal and Inland Stations, *Journal of Geophysical Research:  
824 Atmospheres*, 109, 2004.
- 825 **Haus, N., Schaefer, C. E., Bockheim, J., and Pereira, T. T. C.:** Soils of Graham and Palmer Lands, Antarctic  
826 Peninsula, in: *The Soils of Antarctica*, Springer, 205-225, 2015.
- 827 **Hemkemeyer, M., Dohrmann, A. B., Christensen, B. T., and Tebbe, C. C. J. F. i. m.:** Bacterial Preferences for  
828 Specific Soil Particle Size Fractions Revealed by Community Analyses, 9, 149, 2018.
- 829 **Hjort, C., Ingólfsson, Ó., Möller, P., and Lirio, J. M.:** Holocene Glacial History and Sea-Level Changes on  
830 James Ross Island, Antarctic Peninsula, *Journal of Quaternary Science*, 12, 259-273, 1997.
- 831 **Holmgren, G. G.:** A Rapid Citrate-Dithionite Extractable Iron Procedure, *Soil Science Society of America  
832 Journal*, 31, 210-211, 1967.
- 833 **Hrbáček, F., Láska, K., and Engel, Z.:** Effect of Snow Cover on the Active-Layer Thermal Regime—a Case Study  
834 from James Ross Island, Antarctic Peninsula, *Permafrost and Periglacial Processes*, 2016a.
- 835 **Hrbáček, F., Láska, K., Nývlt, D., Engel, Z., and Oliva, M.:** Active Layer Thickness Variability on James Ross  
836 Island, Eastern Antarctic Peninsula, *International Conference on Permafrost*, Potsdam, Germany, 2016b,
- 837 **Hrbáček, F., Oliva, M., Láska, K., Ruiz-Fernández, J., Pablo, M. Á. D., Vieira, G., Ramos, M., and Nývlt,  
838 D.:** Active Layer Thermal Regime in Two Climatically Contrasted Sites of the Antarctic Peninsula  
839 Region, *Cuadernos de Investigación Geográfica*, 42(2), 451-474, 10.18172/cig.2915, 2016c.
- 840 **Hrbáček, F., Kňázková, M., Nývlt, D., Láska, K., Mueller, C. W., and Ondruch, J.:** Active Layer Monitoring  
841 at Calm-S Site near J.G.Mendel Station, James Ross Island, Eastern Antarctic Peninsula, *Science of The  
842 Total Environment*, 601, 987-997, <http://dx.doi.org/10.1016/j.scitotenv.2017.05.266>, 2017a.
- 843 **Hrbáček, F., Nývlt, D., and Láska, K.:** Active Layer Thermal Dynamics at Two Lithologically Different Sites  
844 on James Ross Island, Eastern Antarctic Peninsula, *Catena*, 149, Part 2, 592-602,  
845 <http://dx.doi.org/10.1016/j.catena.2016.06.020>, 2017b.
- 846 **IUSS Working Group WRB:** World Reference Base for Soil Resources 2014, Update 2015 International Soil  
847 Classification System for Naming Soils and Creating Legends for Soil Maps, *World Soil Resources  
848 Reports* edited by: FAO, Rome, 2015.
- 849 **Jensen, H. I.:** Report on Antarctic Soils, *Reports of Geology* 2, Expedition, 1916.
- 850 **Ji, M., Greening, C., Vanwonterghem, I., Carere, C. R., Bay, S. K., Steen, J. A., Montgomery, K., Lines, T.,  
851 Beardall, J., and van Dorst, J.:** Atmospheric Trace Gases Support Primary Production in Antarctic  
852 Desert Surface Soil, *Nature*, 552, 400, 2017.
- 853 **Kaiser, K., and Guggenberger, G.:** The Role of Dom Sorption to Mineral Surfaces in the Preservation of Organic  
854 Matter in Soils, *Organic geochemistry*, 31, 711-725, 2000.



- 855 **Kirshner, A. E., and Anderson, J. B.:** Cenozoic Glacial History of the Northern Antarctic Peninsula: A  
856 Micromorphological Investigation of Quartz Sand Grains, Tectonic, climatic, and cryospheric evolution  
857 of the Antarctic Peninsula, 153-165, 2011.
- 858 **Könneke, M., Schubert, D. M., Brown, P. C., Hügler, M., Standfest, S., Schwander, T., von Borzyskowski,  
859 L. S., Erb, T. J., Stahl, D. A., and Berg, I. A.:** Ammonia-Oxidizing Archaea Use the Most Energy-  
860 Efficient Aerobic Pathway for Co<sub>2</sub> Fixation, *Proceedings of the National Academy of Sciences*,  
861 201402028, 2014.
- 862 **Kronberg, B., and Nesbitt, H.:** Quantification of Weathering, *Soil Geochemistry and Soil Fertility*, *European  
863 Journal of Soil Science*, 32, 453-459, 1981.
- 864 **Kühn, P., Lehdorff, E., and Fuchs, M.:** Lateglacial to Holocene Pedogenesis and Formation of Colluvial  
865 Deposits in a Loess Landscape of Central Europe (Wetterau, Germany), *Catena*, 154, 118-135, 2017.
- 866 **Láska, K., Barták, M., Hájek, J., Prošek, P., and Bohuslavová, O.:** Climatic and Ecological Characteristics of  
867 Deglaciated Area of James Ross Island, Antarctica, with a Special Respect to Vegetation Cover, *Czech  
868 Polar Reports*, 1, 49-62, 2011.
- 869 **Láska, K., Nývlt, D., Engel, Z., and Budík, L.:** Seasonal Variation of Meteorological Variables and Recent  
870 Surface Ablation/Accumulation Rates on Davies Dome and Whisky Glacier, James Ross Island,  
871 Antarctica, *EGU General Assembly Conference Abstracts*, 2012, 5545,
- 872 **Liebner, S., Harder, J., and Wagner, D.:** Bacterial Diversity and Community Structure in Polygonal Tundra  
873 Soils from Samoylov Island, Lena Delta, Siberia, *International Microbiology*, 11, 195-202, 2008.
- 874 **Ma, G.-Y., He, L.-Y., and Sheng, X.-F.:** Characterization of Bacterial Community Inhabiting the Surfaces of  
875 Weathered Bricks of Nanjing Ming City Walls, *Science of the Total Environment*, 409, 756-762, 2011.
- 876 **Magalhães, C. M., Machado, A., Frank-Fahle, B., Lee, C. K., and Cary, S. C.:** The Ecological Dichotomy of  
877 Ammonia-Oxidizing Archaea and Bacteria in the Hyper-Arid Soils of the Antarctic Dry Valleys,  
878 *Frontiers in microbiology*, 5, 515, 2014.
- 879 **Martin, M.:** Cutadapt Removes Adapter Sequences from High-Throughput Sequencing Reads, *EMBnet journal*,  
880 17, pp. 10-12, 2011.
- 881 **Martin, P., and Peel, D.:** The Spatial Distribution of 10 M Temperatures in the Antarctic Peninsula, *Journal of  
882 Glaciology*, 20, 311-317, 1978.
- 883 **Michel, R. F., Schaefer, C. E., López-Martínez, J., Simas, F. N., Haus, N. W., Serrano, E., and Bockheim, J.  
884 G.:** Soils and Landforms from Fildes Peninsula and Ardley Island, Maritime Antarctica, *Geomorphology*,  
885 225, 76-86, 2014.
- 886 **Mirabella, A., and Carnicelli, S.:** Iron Oxide Mineralogy in Red and Brown Soils Developed on Calcareous  
887 Rocks in Central Italy, *Geoderma*, 55, 95-109, 1992.
- 888 **Moura, P. A., Francelino, M. R., Schaefer, C. E. G. R., Simas, F. N. B., and de Mendonça, B. A. F.:**  
889 Distribution and Characterization of Soils and Landform Relationships in Byers Peninsula, Livingston  
890 Island, Maritime Antarctica, *Geomorphology*, 155-156, 45-54,  
891 <https://doi.org/10.1016/j.geomorph.2011.12.011>, 2012.
- 892 **Müller, V., and Oren, A.:** Metabolism of Chloride in Halophilic Prokaryotes, *Extremophiles*, 7, 261-266, 2003.
- 893 **Muyzer, G., De Waal, E. C., and Uitterlinden, A. G.:** Profiling of Complex Microbial Populations by Denaturing  
894 Gradient Gel Electrophoresis Analysis of Polymerase Chain Reaction-Amplified Genes Coding for 16S  
895 Rrna, *Applied and environmental microbiology*, 59, 695-700, 1993.



- 896 **Nedbalová, L., Nývlt, D., Kopáček, J., Šobr, M., and Elster, J.:** Freshwater Lakes of Ulu Peninsula, James Ross  
897 Island, North-East Antarctic Peninsula: Origin, Geomorphology and Physical and Chemical Limnology,  
898 Antarctic Science, 25, 358-372, 10.1017/S0954102012000934, 2013.
- 899 **Nesbitt, H., and Young, G.:** Early Proterozoic Climates and Plate Motions Inferred from Major Element  
900 Chemistry of Lutites, Nature, 299, 715-717, 1982.
- 901 **Niederberger, T. D., Sohm, J. A., Gunderson, T., Tirindelli, J., Capone, D. G., Carpenter, E. J., and Cary,  
902 S. C.:** Carbon-Fixation Rates and Associated Microbial Communities Residing in Arid and Ephemeral  
903 Wet Antarctic Dry Valley Soils, Frontiers in microbiology, 6, 1347, 2015.
- 904 **Nývlt, D., Braucher, R., Engel, Z., and Mlčoch, B.:** Timing of the Northern Prince Gustav Ice Stream Retreat  
905 and the Deglaciation of Northern James Ross Island, Antarctic Peninsula During the Last Glacial–  
906 Interglacial Transition, Quaternary Research, 82, 441-449,  
907 <http://dx.doi.org/10.1016/j.yqres.2014.05.003>, 2014.
- 908 **Nývlt, D., Fišáková, M. N., Barták, M., Stachoň, Z., Pavel, V., Mlčoch, B., and Láška, K.:** Death Age,  
909 Seasonality, Taphonomy and Colonization of Seal Carcasses from Ulu Peninsula, James Ross Island,  
910 Antarctic Peninsula, Antarctic Science, 28, 3-16, 2016.
- 911 **Oren, A.:** Diversity of Halophilic Microorganisms: Environments, Phylogeny, Physiology, and Applications,  
912 Journal of Industrial Microbiology and Biotechnology, 28, 56-63, 2002.
- 913 **Parnikoza, I., Abakumov, E., Korsun, S., Klymenko, I., Netsyk, M., Kudinova, A., and Kozeretska, I.:** Soils  
914 of the Argentine Islands, Antarctica: Diversity and Characteristics, herausgegeben vom Alfred-Wegener-  
915 Institut Helmholtz-Zentrum für Polar-und Meeresforschung und der Deutschen Gesellschaft für  
916 Polarforschung e. V., 83, 2017.
- 917 **Pearce, D. A., Newsham, K., Thorne, M., Calvo-Bado, L., Krsek, M., Laskaris, P., Hodson, A., and  
918 Wellington, E. M.:** Metagenomic Analysis of a Southern Maritime Antarctic Soil, Frontiers in  
919 Microbiology, 3, 403, 2012.
- 920 **Pereira, T. T. C., Schaefer, C. E. G. R., Ker, J. C., Almeida, C. C., and Almeida, I. C. C.:** Micromorphological  
921 and Microchemical Indicators of Pedogenesis in Ornithogenic Cryosols (Gelisols) of Hope Bay, Antarctic  
922 Peninsula, Geoderma, 193–194, 311-322, <http://dx.doi.org/10.1016/j.geoderma.2012.10.023>, 2013.
- 923 **Pereira, J. L., Pereira, P., Padeiro, A., Gonçalves, F., Amaro, E., Leppe, M., Verkulich, S., Hughes, K. A.,  
924 Peter, H.-U., and Canário, J.:** Environmental Hazard Assessment of Contaminated Soils in Antarctica:  
925 Using a Structured Tier 1 Approach to Inform Decision-Making, Science of The Total Environment, 574,  
926 443-454, <https://doi.org/10.1016/j.scitotenv.2016.09.091>, 2017.
- 927 **Ramnarine, R., Voroney, R., Wagner-Riddle, C., and Dunfield, K.:** Carbonate Removal by Acid Fumigation  
928 for Measuring the  $\Delta 13c$  of Soil Organic Carbon, Canadian Journal of Soil Science, 91, 247-250, 2011.
- 929 **Russell, L. M., Hawkins, L. N., Frossard, A. A., Quinn, P. K., and Bates, T. S.:** Carbohydrate-Like  
930 Composition of Submicron Atmospheric Particles and Their Production from Ocean Bubble Bursting,  
931 Proceedings of the National Academy of Sciences, 107, 6652-6657, 2010.
- 932 **Salzmann, U., Riding, J. B., Nelson, A. E., and Smellie, J. L.:** How Likely Was a Green Antarctic Peninsula  
933 During Warm Pliocene Interglacials? A Critical Reassessment Based on New Palynofloras from James  
934 Ross Island, Palaeogeography, Palaeoclimatology, Palaeoecology, 309, 73-82,  
935 <http://dx.doi.org/10.1016/j.palaeo.2011.01.028>, 2011.



- 936 **Schaefer, C. E. G. R., Simas, F. N. B., Gilkes, R. J., Mathison, C., da Costa, L. M., and Albuquerque, M. A.:**  
937 Micromorphology and Microchemistry of Selected Cryosols from Maritime Antarctica, *Geoderma*, 144,  
938 104-115, <http://dx.doi.org/10.1016/j.geoderma.2007.10.018>, 2008.
- 939 **Schaefer, C. E. G. R., Pereira, T. T. C., Almeida, I. C. C., Michel, R. F. M., Corrêa, G. R., Figueiredo, L. P.**  
940 **S., and Ker, J. C.:** Penguin Activity Modify the Thermal Regime of Active Layer in Antarctica: A Case  
941 Study from Hope Bay, *CATENA*, 149, 582-591, <https://doi.org/10.1016/j.catena.2016.07.021>, 2017.
- 942 **Schwertmann, U.:** Differenzierung Der Eisenoxide Des Bodens Durch Extraktion Mit Ammoniumoxalat-Lösung,  
943 *Journal of Plant Nutrition and Soil Science*, 105, 194-202, 1964.
- 944 **Shur, Y., Hinkel, K. M., and Nelson, F. E.:** The Transient Layer: Implications for Geocryology and Climate-  
945 Change Science, *Permafrost and Periglacial Processes*, 16, 5-17, 10.1002/ppp.518, 2005.
- 946 **Siciliano, S. D., Palmer, A. S., Winsley, T., Lamb, E., Bissett, A., Brown, M. V., van Dorst, J., Ji, M., Ferrari,**  
947 **B. C., and Grogan, P.:** Soil Fertility Is Associated with Fungal and Bacterial Richness, Whereas Ph Is  
948 Associated with Community Composition in Polar Soil Microbial Communities, *Soil Biology and*  
949 *Biochemistry*, 78, 10-20, 2014.
- 950 **Sigler, W., Crivii, S., and Zeyer, J.:** Bacterial Succession in Glacial Forefield Soils Characterized by Community  
951 Structure, Activity and Opportunistic Growth Dynamics, *Microbial Ecology*, 44, 306-316, 2002.
- 952 **Simas, F. N. B., Schaefer, C. E. G. R., Filho, M. R. A., Francelino, M. R., Filho, E. I. F., and da Costa, L. M.:**  
953 Genesis, Properties and Classification of Cryosols from Admiralty Bay, Maritime Antarctica, *Geoderma*,  
954 144, 116-122, <http://dx.doi.org/10.1016/j.geoderma.2007.10.019>, 2008.
- 955 **Simas, F. N., Schaefer, C. E., Michel, R. F., Francelino, M. R., and Bockheim, J. G.:** Soils of the South Orkney  
956 and South Shetland Islands, Antarctica, in: *The Soils of Antarctica*, Springer, 227-273, 2015.
- 957 **Šmilauer, P., and Lepš, J.:** *Multivariate Analysis of Ecological Data Using Canoco 5*, Cambridge university  
958 press, 2014.
- 959 **Souza, K. K. D., Schaefer, C. E. G., Simas, F. N. B., Spinola, D. N., and de Paula, M. D.:** Soil Formation in  
960 Seymour Island, Weddell Sea, Antarctica, *Geomorphology*, 225, 87-99, 2014.
- 961 **Spinola, D. N., Portes, R. d. C., Schaefer, C. E. G. R., Solleiro-Rebolledo, E., Pi-Puig, T., and Kühn, P.:**  
962 Eocene Paleosols on King George Island, Maritime Antarctica: Macromorphology, Micromorphology  
963 and Mineralogy, *CATENA*, 152, 69-81, <http://dx.doi.org/10.1016/j.catena.2017.01.004>, 2017.
- 964 **Stoops, G.:** Guidelines for Analysis and Description of Soil and Regolith Thin Sections, Soil Science Society of  
965 America Inc., 2003.
- 966 **Udisti, R., Dayan, U., Becagli, S., Busetto, M., Frosini, D., Legrand, M., Lucarelli, F., Preunkert, S., Severi,**  
967 **M., and Traversi, R.:** Sea Spray Aerosol in Central Antarctica. Present Atmospheric Behaviour and  
968 Implications for Paleoclimatic Reconstructions, *Atmospheric environment*, 52, 109-120, 2012.
- 969 **Ugolini, F.:** A Study of Pedogenic Processes in Antarctica, Final report to the National Science Foundation,  
970 Rutgers University, New Brunswick, NJ, 1964.
- 971 **Ugolini, F. C., and Bockheim, J. G.:** Antarctic Soils and Soil Formation in a Changing Environment: A Review,  
972 *Geoderma*, 144, 1-8, <http://dx.doi.org/10.1016/j.geoderma.2007.10.005>, 2008.
- 973 **Uroz, S., Calvaruso, C., Turpault, M.-P., and Frey-Klett, P.:** Mineral Weathering by Bacteria: Ecology, Actors  
974 and Mechanisms, *Trends in Microbiology*, 17, 378-387, <http://dx.doi.org/10.1016/j.tim.2009.05.004>,  
975 2009.



- 976 **Vajrala, N., Martens-Habbena, W., Sayavedra-Soto, L. A., Schauer, A., Bottomley, P. J., Stahl, D. A., and**  
977 **Arp, D.:** Hydroxylamine as an Intermediate in Ammonia Oxidation by Globally Abundant Marine  
978 Archaea, *Proceedings of the National Academy of Sciences*, 110, 1006-1011, 2013.
- 979 **Van Vliet-Lanoë, B.:** Frost Effects in Soils, *Soils and quaternary landscape evolution*, 117-158, 1985.
- 980 **Van Vliet-Lanoë, B., Fox, C. A., and Gubin, S. V.:** Micromorphology of Cryosols, in: *Cryosols*, Springer, 365-  
981 390, 2004.
- 982 **Van Vliet-Lanoë, B.:** Frost Action-6, in: *Interpretation of Micromorphological Features of Soils and Regoliths*,  
983 edited by: Stoops, G., Marcelino, V., and Mees, F., Elsevier, Amsterdam, The Netherlands, 2010.
- 984 **Wilhelm, K. R., Bockheim, J. G., and Haus, N. W.:** Properties and Processes of Recently Established Soils from  
985 Deglaciation of Cierva Point, Western Antarctic Peninsula, *Geoderma*, 277, 10-22,  
986 <https://doi.org/10.1016/j.geoderma.2016.05.001>, 2016.
- 987 **Yergeau, E., Newsham, K. K., Pearce, D. A., and Kowalchuk, G. A.:** Patterns of Bacterial Diversity across a  
988 Range of Antarctic Terrestrial Habitats, *Environmental microbiology*, 9, 2670-2682, 2007.
- 989 **Zeng, Y., Selyanin, V., Lukeš, M., Dean, J., Kaftan, D., Feng, F., and Koblížek, M.:** Characterization of the  
990 Microaerophilic, Bacteriochlorophyll a-Containing Bacterium *Gemmatimonas Phototrophica* Sp. Nov.,  
991 and Emended Descriptions of the Genus *Gemmatimonas* and *Gemmatimonas Aurantiaca*, *International*  
992 *journal of systematic evolutionary microbiology*, 65, 2410-2419, 2015.
- 993 **Zhang, J., Kobert, K., Flouri, T., and Stamatakis, A.:** Pear: A Fast and Accurate Illumina Paired-End Read  
994 Merger, *Bioinformatics*, 30, 614-620, 2013.
- 995 **Zvěřina, O., Láska, K., Červenka, R., Kuta, J., Coufalík, P., and Komárek, J.:** Analysis of Mercury and Other  
996 Heavy Metals Accumulated in Lichen *Usnea Antarctica* from James Ross Island, Antarctica,  
997 *Environmental Monitoring and Assessment*, 186, 9089-9100, [10.1007/s10661-014-4068-z](https://doi.org/10.1007/s10661-014-4068-z), 2014.
- 998  
999



1000 **Tables**

1001 **Table 1: Soil properties of two soil profiles from St. Marta Cove (SMC) and Brandy Bay (BB) from James Ross Island,**  
 1002 **Antarctica.**

Sample	Depth [cm]	pH <sub>H2O</sub>	EC [μS cm <sup>-1</sup> ]	TIC [%]	TOC [mg g <sup>-1</sup> ]	N [mg g <sup>-1</sup> ]	C/N	K <sup>+</sup> [μmol g <sup>-1</sup> ]	Mg <sup>+</sup> [μmol g <sup>-1</sup> ]	Ca <sup>+</sup> [μmol g <sup>-1</sup> ]	Cl <sup>-</sup> [μmol g <sup>-1</sup> ]	SO <sub>4</sub> <sup>2-</sup> [μmol g <sup>-1</sup> ]	Sand 63–2000 μm [%]	Silt 2–63 μm [%]	Clay <2 μm [%]
SMC 0-5	0-5	7.7	46	0.01	0.9	0.4	2.6	2.5	4	10.4	20.6	9.6	61.2	18.9	19.8
SMC 5-10	5-10	8	36	0.01	0.9	0.4	2.5	2.4	3.6	9.6	13.1	5.7	59.9	19.4	20.7
SMC 10-20	10-20	7.9	33	0.03	0.9	0.4	2.3	2	3.1	8.3	8.7	3.3	63.8	17.1	19.1
SMC 20-50	20-50	8	33	0.01	0.8	0.4	2.2	1.5	2.1	4.9	5.5	3	61.9	17.2	20.8
SMC >50	>50	8.1	65	0.02	0.9	0.4	2.1	2.7	3.1	6.3	3.5	15.3	61.7	20	18.3
BB 0-5	0-5	8.6	950	0.14	1.4	0.4	4	23.4	84.6	151	4522	621	49.8	25.2	24.9
BB 5-10	5-10	8.1	561	0.12	2.1	0.4	5.6	16.3	57.4	108	702	123	46.4	25.7	27.9
BB 10-20	10-20	7.7	385	0.07	2	0.3	5.9	12.2	42.6	93	369	88	52.5	21.9	25.6
BB 20-50	20-50	7.6	505	0.2	2.5	0.4	6.7	18.3	79.8	173	386	163	44	27.2	28.8
BB >50	>50	7.4	965	0.1	2.6	0.4	7.4	23.9	140	297	231	451	44.3	26.8	28.9

1003  
 1004  
 1005



1006 **Table 2: Weathering indices (WI) and pedogenic oxide ratios (POR) of two soil profiles from St. Marta Cove (SMC)**  
 1007 **and Brandy Bay (BB) from James Ross Island, Antarctica. CIA = chemical index of alteration; KN-A = Kronberg**  
 1008 **Nesbitt Index; Fe<sub>d</sub> = dithionite-soluble iron; Fe<sub>t</sub> = total iron; Fe<sub>o</sub> = oxalate-soluble iron.**

Sample	Depth [cm]	WI		POR				
		CIA	KN-A	Fe <sub>d</sub> /Fe <sub>t</sub>	Fe <sub>o</sub> /Fe <sub>d</sub>	Fe <sub>t</sub> [mg g <sup>-1</sup> ]	Fe <sub>d</sub> [mg g <sup>-1</sup> ]	Fe <sub>o</sub> [mg g <sup>-1</sup> ]
SMC 0-5	0-5	53.9	0.92	0.18	0.56	45.57	7.99	4.48
SMC 5-10	5-10	54.2	0.91	0.18	0.45	44.71	7.83	3.56
SMC 10-20	10-20	54.8	0.91	0.16	0.53	40.74	6.61	3.48
SMC 20-50	20-50	54.3	0.91	0.15	0.59	40.76	5.96	3.53
SMC > 50	>50	54.1	0.92	0.11	1.72	42.25	4.83	8.3
BB 0-5	0-5	56.9	0.89	0.16	0.61	53.77	8.68	5.3
BB 5-10	5-10	58.5	0.89	0.21	0.57	44.09	9.08	5.19
BB 10-20	10-20	58.1	0.9	0.2	0.58	42.57	8.34	4.85
BB 20-50	20-50	58.8	0.9	0.21	0.56	39.82	8.43	4.68
BB > 50	>50	58.2	0.9	0.21	0.54	38.18	7.88	4.24



1009 **Table 3: Major elements by XRF of two soil profiles from St. Marta Cove (SMC) and Brandy Bay (BB) from James**  
 1010 **Ross Island, Antarctica. Sample names contain information about sample dpth (in cm), LOI (loss on ignition)**  
 1011 **determined at 1000°C.**

Sample	Depth [cm]	SiO <sub>2</sub> [%]	THO <sub>2</sub> [%]	Al <sub>2</sub> O <sub>3</sub> [%]	Fe <sub>2</sub> O <sub>3</sub> [%]	MnO [%]	MgO [%]	CaO [%]	Na <sub>2</sub> O [%]	K <sub>2</sub> O [%]	P <sub>2</sub> O <sub>5</sub> [%]	Ba [mg kg <sup>-1</sup> ]	Rb [mg kg <sup>-1</sup> ]	Sr [mg kg <sup>-1</sup> ]	V [mg kg <sup>-1</sup> ]	Y [mg kg <sup>-1</sup> ]	Zn [mg kg <sup>-1</sup> ]	Zr [mg kg <sup>-1</sup> ]	Eu [mg kg <sup>-1</sup> ]	La [mg kg <sup>-1</sup> ]	LOI [%]	Sum [%]
SMC 0-5	0-5	69.4	1.0	11.6	6.5	0.1	1.9	2.2	1.9	2.7	0.2	514	84	280	111	58	0	717	0.9	40	2.68	100.3
SMC 5-10	5-10	69.3	1.0	11.9	6.4	0.2	1.9	2.3	1.9	2.6	0.2	521	80	303	117	55	0	759	0.9	35	2.77	100.5
SMC 10-20	10-20	70.1	0.9	12.1	5.8	0.1	1.5	2.0	2.0	2.9	0.1	539	90	285	105	46	0	628	0.9	33	3.36	101.0
SMC 20-50	20-50	69.6	0.9	12.2	5.8	0.1	1.8	2.2	2.0	2.7	0.1	528	87	276	110	49	0	564	0.9	30	2.73	100.5
SMC > 50	>50	70.2	1.0	11.9	6.0	0.1	1.6	2.1	2.0	2.8	0.1	545	87	320	110	39	0	644	0.9	36	2.51	100.6
BB 0-5	0-5	60.5	1.1	14.5	7.7	0.2	3.4	3.7	2.5	2.0	0.3	456	62	362	135	38	14	339	1.0	21	4.26	100.2
BB 5-10	5-10	64.5	0.9	14.2	6.3	0.1	2.3	2.5	1.9	2.4	0.2	502	83	266	112	37	8	390	0.9	19	5.83	101.4
BB 10-20	10-20	65.5	0.9	13.9	6.1	0.1	2.4	2.6	2.0	2.4	0.2	500	83	315	111	24	5	346	0.9	21	4.16	100.4
BB 20-50	20-50	66.3	0.9	14.2	5.7	0.1	2.0	2.1	1.8	2.6	0.1	522	95	240	106	44	0	629	0.8	22	4.50	100.5
BB > 50	>50	65.1	0.8	13.7	5.5	0.1	2.0	2.9	1.8	2.6	0.1	502	92	262	101	35	0	655	0.9	14	5.47	100.2

1012  
 1013



1014 **Table 4: Micromorphological features of two soil profiles from St. Marta Cove (SMC) and Brandy Bay (BB) from James**  
 1015 **Ross Island, Antarctica**  
 1016 **The micromorphological property is shown by the presence (cross) or absence (no cross). (x) = occasional occurring**  
 1017 **\* Microstructures separated by "/": two different microstructures were found. Microstructures separated by "()": one**  
 1018 **ms shows partly features of another ms**  
 1019 **\*\* Degree of roundness and sphericity results separated by "'": two different degrees were mainly present ; measured**  
 1020 **at 10x magnification.**

Slide	Depth	Aggregation		Voids		Micros *		Groundmass		Pedofeatures															
		wp	mp	hp	ds	spv	xpv	pl	vu	cm	cg	oec	sse	chi	ce	color	b-Fabric	nodules	hp	ro	li	cap	pen	ld	
		Pedality				RS**		cf - related distribution		Micromass		Redoximorphic features		Translocation features											
SMC I	0-10	x			w	(x)	x	(x)	sub/su	x	(x)	(x)		gb	x		x	(x)	(x)			(x)			
SMC II	10-20		x		w	(x)	x	(x)	su	x		x		gb	x		x					x			
SMC III	30-40		(x)		w/m		x		sub/su	x	(x)	x		db	x	x	x				x				x
SMC IV	50-60		x		m/w		x	(x)	sub/su	x	x	x		db	x	x	x				x	(x)			x
SMC V	80-90		x		w		x	(x)	sub/su	x	(x)	x		db	x	(x)									
BB I	10-20		(x)		m		x	(x)	h-m sp	(x)	x	x	(x)	gb	x	(x)	x				(x)				x
BB II	20-30		x		m		x	x	w-m sp (msl)	sh-ro	(x)	x	(x)	gb	x	x	x	(x)			x				x
BB III	40-50		x		m/h		x	x	h-m sp (msl)	subro	x	x	x	gb	x	x	x				x				x

**Aggregation**  
 : hp = highly developed pedality, mp = moderately developed pedality, wp = weakly developed pedality  
 ds = degree of separation, h = highly separated, m = moderately separated, w = weakly separated  
 : spv = simple packing voids, xpv = complex packing voids, pl = planes, vu = vughs

**Voids**  
 Microstructure \*(Micros) : fs = fissure, sgn = single grain ms, pgn = pelletular grain ms, wsl = weakly separated lenticular ms, hsp = highly separated platy ms  
 : msp = moderately separated platy ms, wsp = weakly separated platy ms, msl = moderately separated lenticular ms

**Groundmass**  
 RS - Degree of Roundness and Sphericity\*\* : sub = subrounded, su = subangular, ro = rounded, su-ro = subangular to rounded mineral grains  
 cf - Related Distribution (cf - R. Distr.) : cm = coarse monic, cg = chito-gefuric, oec = open equal enaulic, ssee = single spaced equal enaulic, chi = chitonic, ce = close enaulic  
 color : gb = greyish brown, db = dark brown  
 b - Fabric : u = undifferentiated, gs = granostriated  
**Pedofeatures**  
 modules : t = typical, a = aggregate  
 hp (typocoatings) : ro = redoximorphic typocoatings  
 coatings : li = link cappings, cap = cappings, pen = pendent  
 infillings : ld = loose discontinuous

1021  
 1022



1023 **Figures**



1024  
1025 **Figure 1: Regional setting of James Ross Island, Maritime Antarctica. Blue symbols indicate the location of both study**  
1026 **sites, Brandy Bay (BB) and St. Marta Cove (SMC). Image credit: Contains modified Copernicus Sentinel data (2016),**  
1027 **processed by ESA, CC BY-SA 3.0 IGO. Map credit: Contains modified OpenStreetMap data (2016), CC BY-SA**  
1028 **[www.openstreetmap.org/copyright](http://www.openstreetmap.org/copyright)).**



1029

1030

**Figure 2: Study site St. Marta Cove (SMC). It is not covered with vegetation. A 90 cm deep soil profile was taken.**



1031

1032

1033

**Figure 3: Study site Brandy Bay (BB) is close to snowfield. It is not covered with vegetation. A 60cm soil profile was taken.**



1034

1035 **Figure 4: Soil profile St. Marta Cove (SMC). Scale of the tape measure is in cm.**

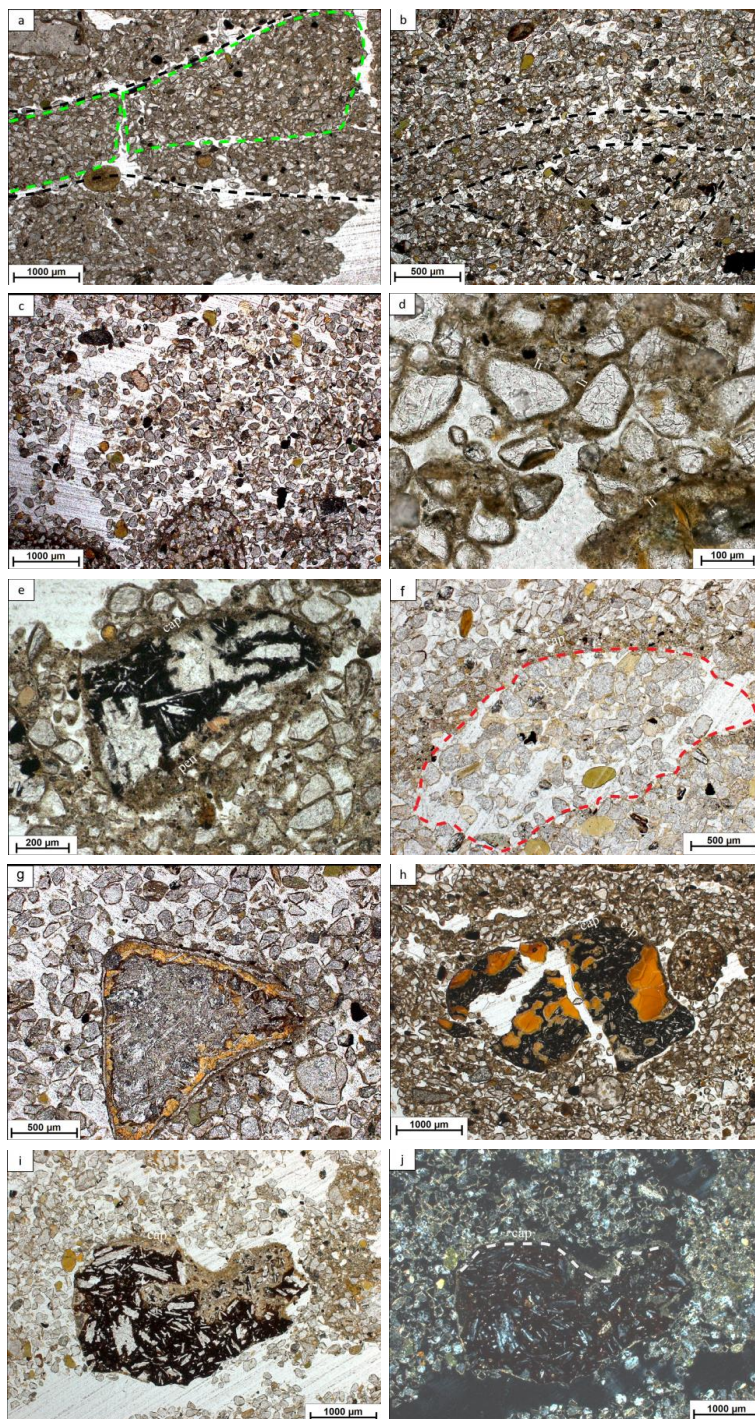


1036

1037 **Figure 5: Soil profile Brandy Bay (BB). Scale of the tape measure is in cm.**

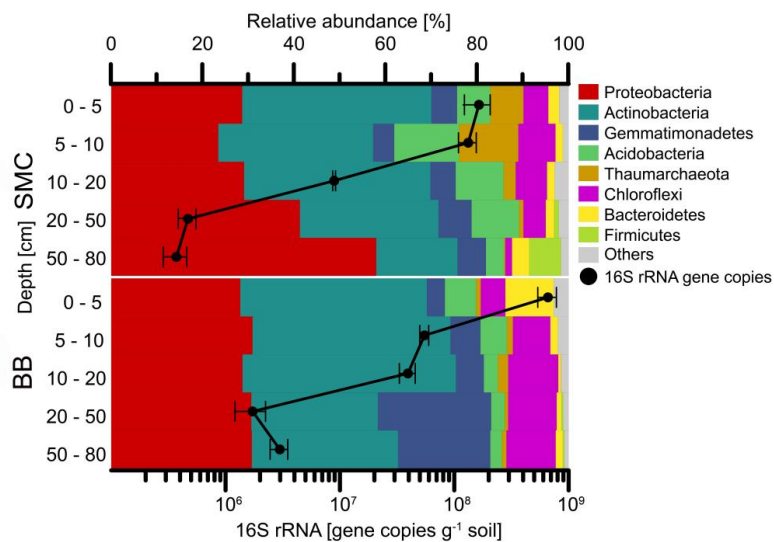


1038  
1039  
1040  
1041  
1042  
1043  
1044  
1045  
1046  
1047  
1048  
1049  
1050  
1051  
1052  
1053  
1054  
1055  
1056  
1057  
1058  
1059  
1060  
1061  
1062  
1063  
1064  
1065  
1066  
1067  
1068  
1069  
1070  
1071  
1072  
1073  
1074  
1075  
1076  
1077  
1078  
1079





1080 **Figure 6: Images of micromorphological features found at Brandy Bay (BB) and St. Marta Cove (SMC). Pictures were taking**  
1081 **using plane polarized light (ppl) and crossed polarizers (xpl). (a) BB III: highly separated lenticular platy microstructure, platy**  
1082 **aggregates are indicated by green dotted lines, lenticular ms is indicated by black dotted lines, 2.5x, ppl; (b) SMC IV:**  
1083 **moderately separated lenticular platy microstructure, indicated by black dotted lines, 2.5x, ppl; (c) SMC I: coarse monic**  
1084 **microstructure, 2.5x, ppl; (d) BB II: chitonic c/f-related distribution and thin link cappings (li) on quartz grains, 20x, ppl; (e)**  
1085 **BB III: weathered rock fragment covered by silty capping (cap) and also showing a thick pendent (pen) consisting of silty**  
1086 **material and mineral grains, 10x, ppl; (f) SMC I: strongly weathered sandstone fragment with former boundaries, indicated**  
1087 **by red dotted line, still visible by capping (cap), 5x, ppl; (g) SMC I: weathered volcanic rock fragment with distinct pellicular**  
1088 **alteration pattern, 5x, ppl; (h) BB II: weathered and broken volcanic rock fragment with internal volcanic glass and covered**  
**by a thin clay capping (cap), (110-120µm), 2.5x, ppl; (i) SMC I: weathered volcanic rock fragment with feldspar phenocrysts;**  
**covered by a dusty clay-silt capping (80-100 µm) (cap), 2.5x, ppl; (j) SMC I: usage of crossed polarizers makes it possible to**  
**tell external coating (cap) from altered internal material, border indicated by grey dotted line, 2.5x, xpl.**



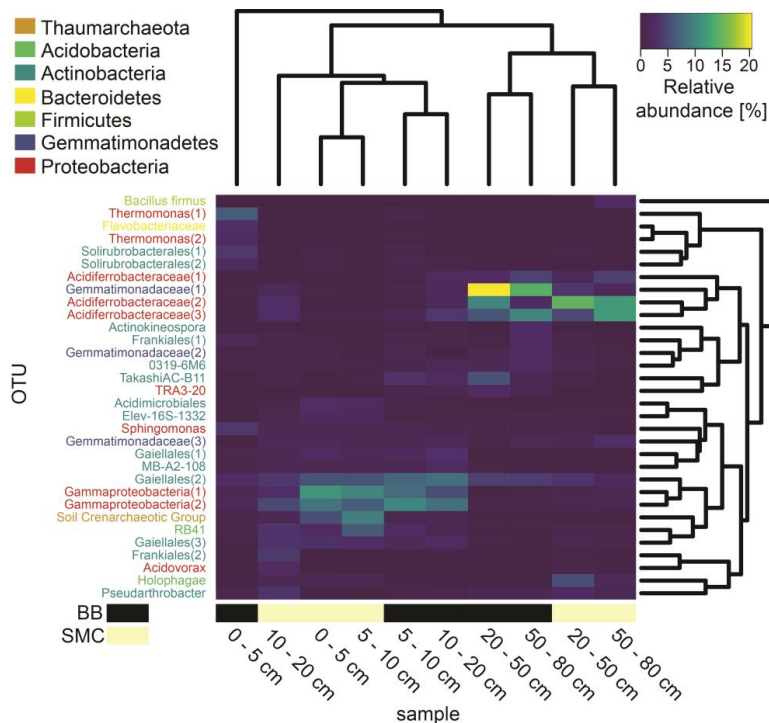
1089

1090

1091

1092

**Figure 7: Relative abundances of phyla and bacterial 16S rRNA qPCR gene abundances of soil profiles from Brandy Bay (BB) and St. Marta Cove (SMC) on James Ross Island, Antarctica. Triplicates are merged. Only phyla with a relative abundance of at least 5% at a given site are shown. The remaining phyla are summarized as “Others”.**



1093

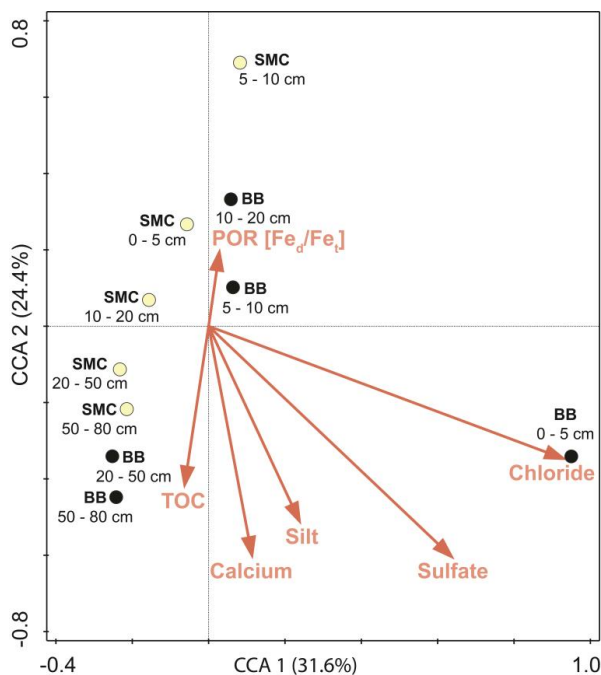
1094

1095

1096

1097

**Figure 8:** Heatmap based on the relative abundances of the observed operational taxonomic units (OTUs) in soil profiles from Brandy Bay (BB) and St. Marta Cove (SMC) on James Ross Island, Antarctica. Only OTUs with a relative abundance of at least 3% in a given sample were included. Samples as well as OTUs were clustered using average linkage hierarchical clustering.



1098

1099

1100

1101

1102

1103

**Figure 9: Canonical correlation analysis of the microbial composition of soil profiles from Brandy Bay (BB; black symbol) and St. Marta Cove (SMC; yellow symbol) based on Bray-Curtis dissimilarities of the OTU data and its associated environmental parameters. If the Bonferroni corrected p-value was below 0.05, a given environmental parameter was included in the visualization. The amounts of chloride, sulfate, silt, Ca and TOC contents, and the Fe<sub>d</sub>/Fe<sub>t</sub> ratio explained 49.9% of the microbial community composition.**